NASA CR-135250

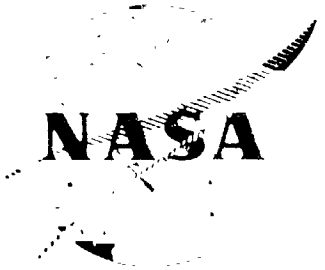

QUIET CLEAN SHORT-HAUL EXPERIMENTAL ENGINE

(QCSEE)

Under-the-Wing (UTW) Engine Boilerplate Nacelle Test Report

VOLUME II

Aerodynamics and Performance

DECEMBER 1977

by

Advanced Engineering and Technology Programs Department

GENERAL ELECTRIC COMPANY

Prepared For

National Aeronautics and Space Administration

NASA Lewis Research Center
NAS3-18021

TABLE OF CONTENTS

LIST OF ILLUSTRATIONS

LIST OF ILLUSTRATIONS (Concluded)

LIST OF TABLES

1.0 SUMMARY

Performance objectives for the UTW propulsion system were established by the Statement of Work as follows:

SLS, 311 K (90° F) day

Uninstalled Thrust	81.4 kN (18,300 lb)
Uninstalled sfc	0.00962 g/sN (0.34 lb/hr/lb)
Installed Thrust	77.4 kN (17,400 lb)

Test data adjusted for ambient conditions at Peebles, Ohio test site met the uninstalled thrust and sfc objectives with a bellmouth inlet, and met the installed thrust objective with a high Mach number inlet. Because of minor deficiencies in the compressor and low pressure turbine efficiencies, the objective T41 levels were exceeded by 31 to 36K (56° - 64° F). These temperatures were well within safe operating limits of the engine. Test data indicated that the exhaust nozzle effective area was about 0.097 m^2 (150 $in.^2$) larger than that calculated from static measurements. Increasing the nozzle area above 1.87 m^2 (2900 $in.^2$) did not affect airflow, indicating that this was the limit of flap divergence without flow separation. Exhaust velocities, which are critical from an acousti standpoint, at the installed takeoff condition were:

Bypass stream	197 m/s (645 ft/sec)
Core stream	256 m/s (840 ft/sec)

Fan performance in the forward operating mode agreed well with scale model simulator data. Airflow exceeded predicted values by 1 - 2% along operating lines near peak efficiencies. Efficiencies were equal to or slightly better than predicted levels. Fan hub performance generally exceeded predicted levels at all blade pitch and speed settings tested, indicating good core supercharging. Although no stall testing was done, stall margin appeared to be adequate for all operating conditions.

The reverse thrust performance objective of 35% of takeoff thrust was not demonstrated due to premature failure of the exhaust nozzle support ring. However, data at off-optimum reverse pitch angle indicated that the reverse thrust objective probably would not have been met at the predicted conditions. Traverse data indicated that the low reverse thrust was due to reduced pressure rise in the fan. As compared to data from the 50.8-cm (20-in.) simulator test fan, rotor airflow and work input appeared to be as expected. The reduced reverse thrust, therefore, is believed to be a result of inlet pressure distortion, perhaps introduced by the acoustic splitter, and possible exhaust gas reingestion effects. These factors will be further investigated on the next engine buildup.

2.0 INTRODUCTION

The General Electric Company currently is engaged in the Quiet Clean, Short-Haul Experimental Engine Program (QCSEE) under Contract NAS3-18021 to the NASA-Lewis Research Center. The under-the-wing (UTW) experimental engine was designed and built under the program to develop and demonstrate technology applicable to engines for future commercial short-haul turbofan aircraft (Reference 1).

The initial buildup of the UTW engine and boilerplate nacelle was tested at the General Electric, Peebles, Ohio Outdoor Test Site 4D during the period from September 2 through December 17, 1976. Initial testing included a mechanical and systems checkout with hardwall acoustic panels and a bellmouth inlet. Performance data were taken over a range of speeds, exhaust nozzle areas, and fan blade angles. This phase of testing provided data in the range of takeoff and approach operating conditions to explore "uninstalled" performance with minimal loss of ram recovery. In addition, fan performance characteristics were mapped over a limited range of blade settings.

The inlet then was changed to the boilerplate high Mach number design to investigate installed performance with real ram recovery losses. Points were repeated at takeoff and approach operating conditions.

Initial reverse thrust testing was attempted by transitioning the blades to the reverse setting (through stall pitch) while motoring on the starter. The engine then was fired in the reverse mode and operated to higher speeds. During this phase of testing, the exhaust nozzle support ring failed, allowing one nozzle flap and associated hardware to be ingested by the engine. This failure resulted in a premature conclusion of the test before much of the desired reverse mode and acoustic data could be acquired.

This volume of the propulsion system test report includes overall propulsion system performance observations and results of detailed analyses of the variable-pitch fan aerodynamic characteristics.

3.0 PROPULSION SYSTEM PERFORMANCE

3.1 FORWARD MODE PERFORMANCE OBJECTIVES

The UTW propulsion system was sized for an 81.4-kN (18,300-lb) thrust, uninstalled, bare engine. It is flat-rated to 311 K (90° F). The performance objective levels as identified in the Statement of Work for sea level static operation are shown in Table 1.

As the QCSEE program progressed, the cycle deck was updated to match current core engine representations. Also, results from scale model QCSEE component tests were factored into the deck. As a result of these revisions, it was predicted that the experimental engine would exceed the objective turbine inlet temperature (T41) levels, since further component development was not scheduled prior to full-scale manufacture. The predicted performance of the nominal experimental engine, as defined by the cycle deck, is included in Table 1.

Another factor, which contributed to increased T41, was found when the engine went to test. At takeoff thrust, the compressor operating point was at a higher flow than expected, and, thus, in a region of low compressor efficiency. The combination of low compressor and LP turbine efficiencies resulted in a higher temperature for a given thrust than planned, although well within engine capability.

It should be noted that engine testing was conducted under local atmospheric conditions at the test site. Any significant fluctuations in ambient conditions during a test reading would result in poor data quality. Where particularly bad data were apparent, they were rejected. However, data from several readings taken under blustery weather conditions were retained because they showed results not otherwise available from the testing. In particular, the installed data at high thrust levels were obtained under adverse weather conditions.

A cross section of the UTW engine showing flow direction in the forward mode is shown in Figure 1. Instrumentation locations are noted on the figure. The acoustic splitter location also is shown in Figure 1, but it was not installed for any of the forward mode performance readings.

3.2 UNINSTALLED PERFORMANCE

As shown in Table 1, on a 311-K (90°-F) day at sea level static, uninstalled, the experimental engine met the sfc goal, but the turbine inlet temperature exceeded the objective by 36 K (64° F). The sfc goal also was met on a standard day, 288.15 K (518.67° R), with the objective T41 level exceeded by 30 K (54° F).

Table 1. UTW Propulsion System Performance Requirements.

	Uninstalled - Bellmouth Inlet			Installed - High Mach Inlet		
	Statement of Work	Nominal Experimental Engine	UTW Engine 507-001/1	Statement of Work	Nominal Experimental Engine	UTW Engine 507-001/1
Takeoff, SLS, 311 K (90° F) Day						
Net Thrust, kN (lbs)	81.4 (18300)	[81.4 (18300)]	[81.4 (18300)]	77.4 (17400)	[77.4 (17400)]	[77.4 (17400)]
sfc, g/sN (lb/hr/lb)	0.00962 (0.34)	[0.00934 (0.33)]	[0.00962 (0.34)]		0.00934 (0.33)	0.00991 (0.35)
Turbine Inlet Temperature Increment, K (° F)	0 (0)	[11 (19)]	[36 (64)]		14 (26)	31 (56)
Bypass Ratio - Approximate	11.8	11.9	11.6		12.0	11.6
Cycle Pressure Ratio - Approximate	13.7	14.5	15.2		14.2	15.2
Takeoff, SLS, Standard Day						
Net Thrust, kN (lbs)	81.4 (18300)	[81.4 (18300)]	[81.4 (18300)]			
sfc, g/sN (lb/hr/lb)	0.00934 (0.33)	[0.00906 (0.32)]	[0.00934 (0.33)]			
Turbine Inlet Temperature Increment, K (° F)	0 (0)	[8 (14)]	[30 (54)]			

Parameters Enclosed in Boxes are Specific Requirements.

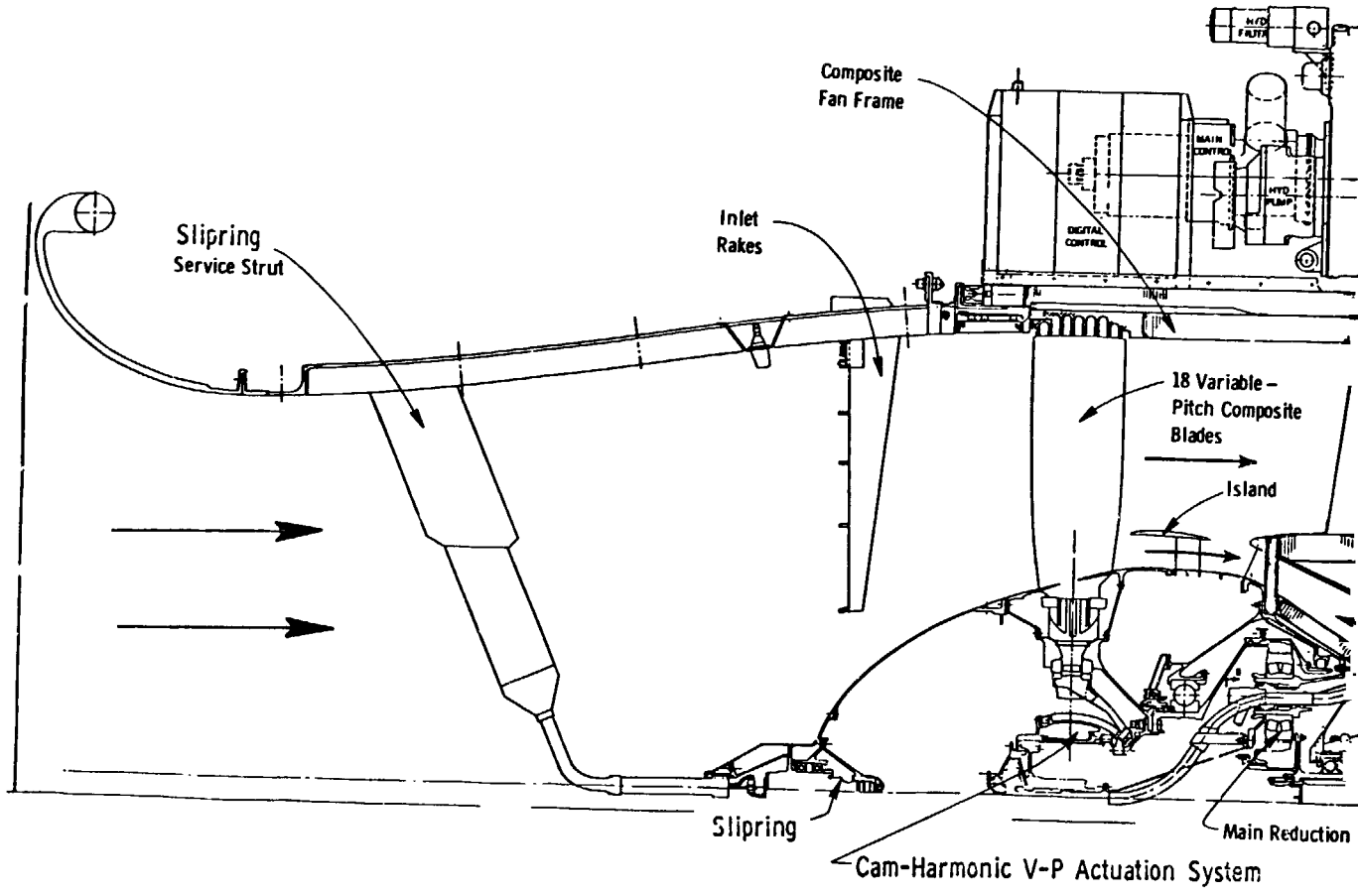

Figure 1. UTW Propulsion System

FOLDOUT FRAME 2

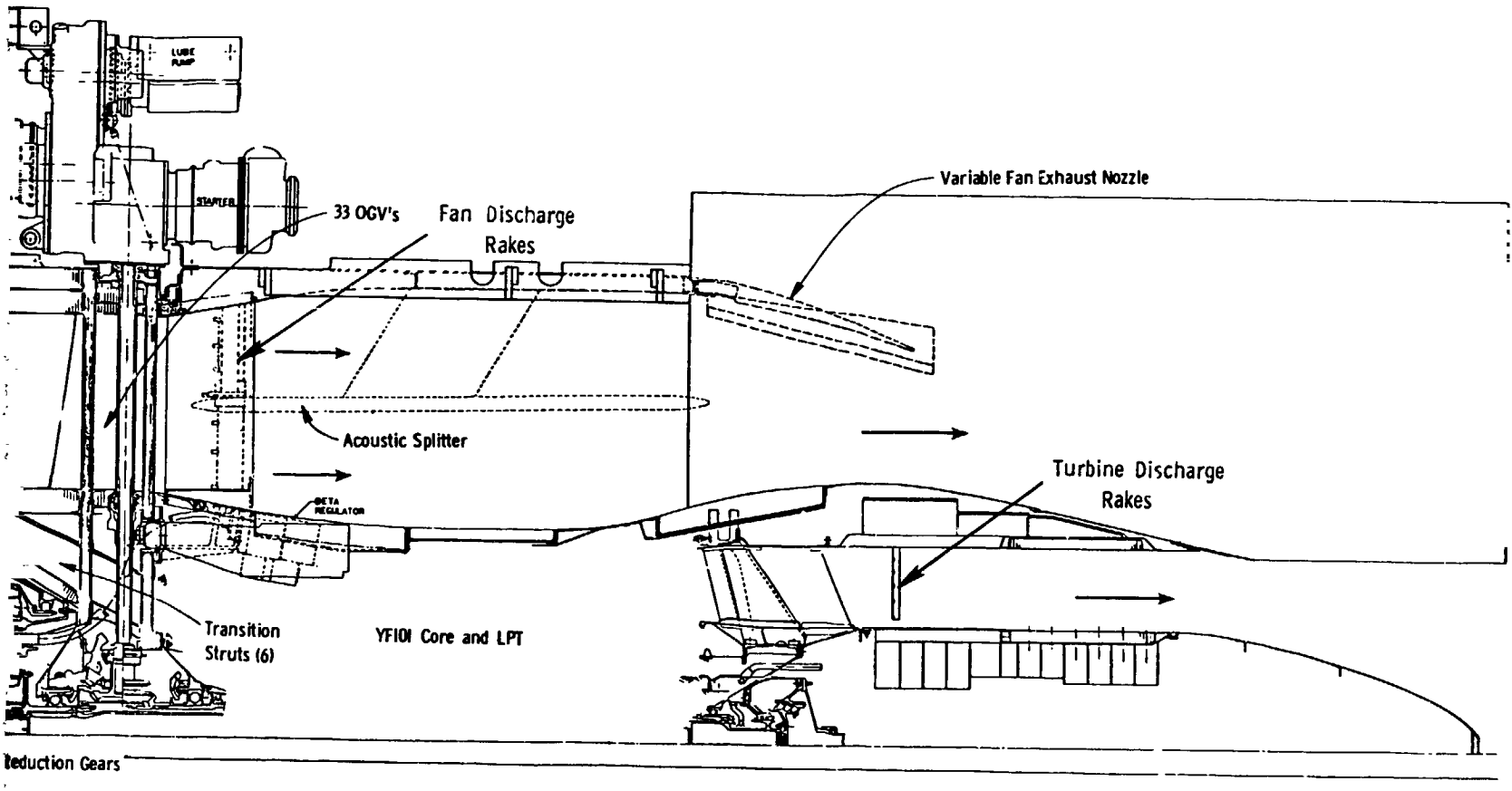

stem Cross Section Showing Forward Mode Flow Direction.

The performance levels for the experimental engine (507-001/1) shown in Table 1 are based on extrapolation from the ambient test conditions at the Peebles test site. The test reading which came closest to matching the objective takeoff performance point was about 1.78 kN (400 lb) low in thrust. This reading was adjusted for the change in ambient conditions and thrust level to get the values shown in Table 1. The fan pitch angle for this reading was -2.8°. There are other possible pitch-setting/fan-speed combinations which also could give takeoff thrust.

3.2.1 Thrust Versus Airflow

Thrust airflow characteristics are shown in Figures 2 through 5 for +5°, 0°, -3°, and -5° pitch angles (ROPDEG), and fan corrected speeds (PCNLR) from 80 to 97%, dependent on data availability. These figures primarily include data from the fan mapping runs. For convenience in making comparisons, the available installed data also are included on these same figures. (The plotting symbols used for the performance plots in this report are shown in the foldout on the last page of Section 3.0.) It was found throughout the testing that the indicated exhaust nozzle area (from static calibrations) was smaller than the calculated (cycle balance) effective area by about 0.097 m^2 (150 $in.^2$) over most of the engine operating range. Data taken at the nominal takeoff area, 1.61 m^2 (2500 $in.^2$), consistently corresponded to the symbols for 1.52 m^2 (2350 $in.^2$) indicated area. Calibration rechecks did not resolve this difference, which probably was due to flap opening under internal pressure or unidentified flow-leakage paths. The engine appeared to be on a lower operating line.

At +5° pitch angle (Figure 2), the measured corrected thrust as a function of corrected airflow tended to be below predictions. At 0° (Figures 2 and 3), the same low trend occurred. At -3° and -5° (Figures 4 and 5), the uninstalled data tend to match predictions more closely.

The trend of thrust versus airflow for all the bellmouth test data above 80% fan speed is shown in Figure 6. The objective uninstalled thrust and takeoff airflow values also are shown.

3.2.2 Specific Fuel Consumption

Specific fuel consumption (sfc) was generally 0.00042 to 0.00057 g/sN (0.015 to 0.02 lb/hr/lb) higher than the predicted minimum. The corrected sfc trends are shown in Figures 7 through 10 for pitch angles +5°, 0°, -3°, -5°, respectively. The data included on these figures are primarily from the fan mapping runs where the bypass nozzle area was varied at constant fan speed. The fuel flow for all the bellmouth data above 80% fan speed is shown in Figure 11.

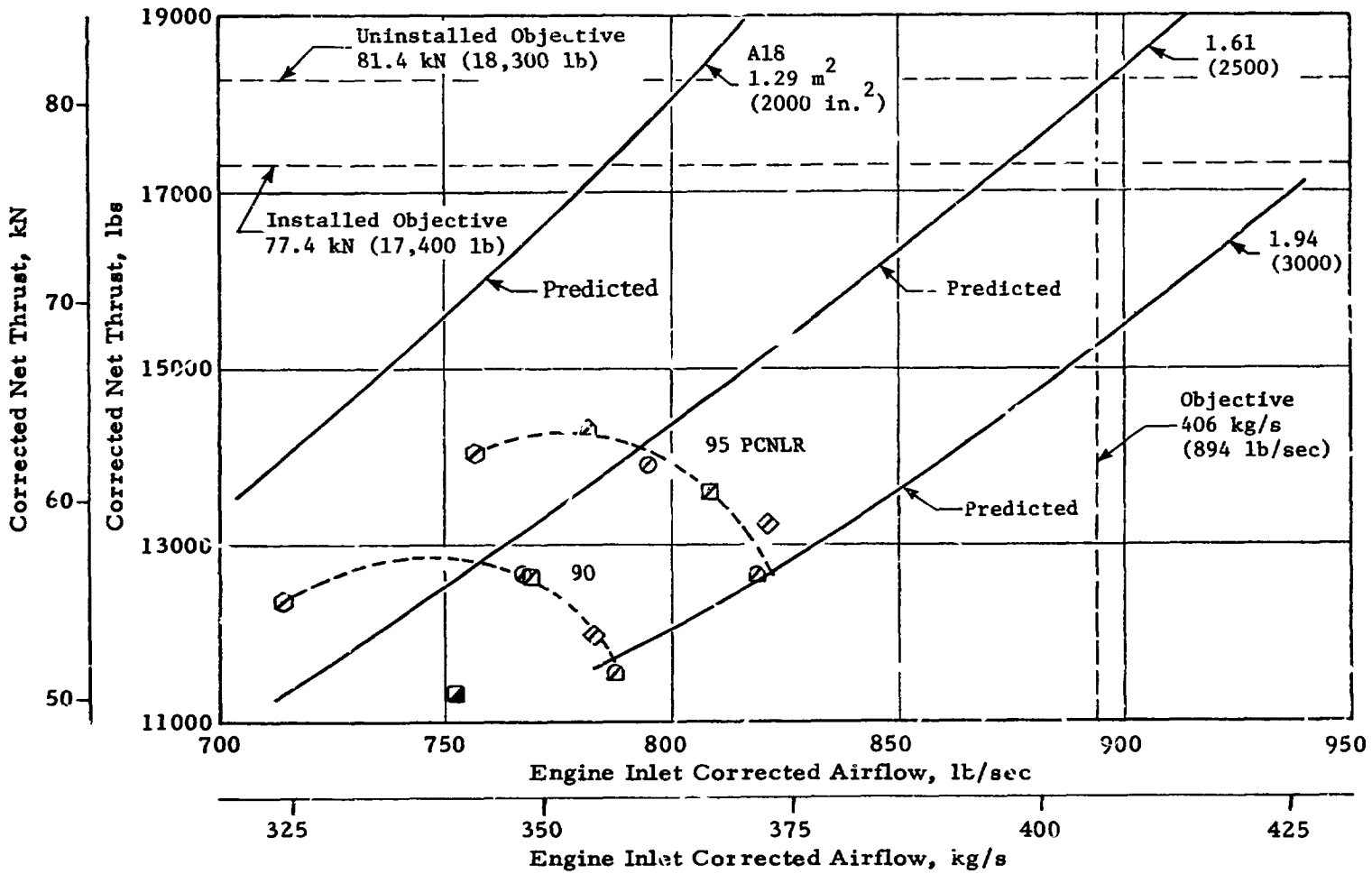

Figure 2. Thrust Versus Airflow, +5° ROPDEG.

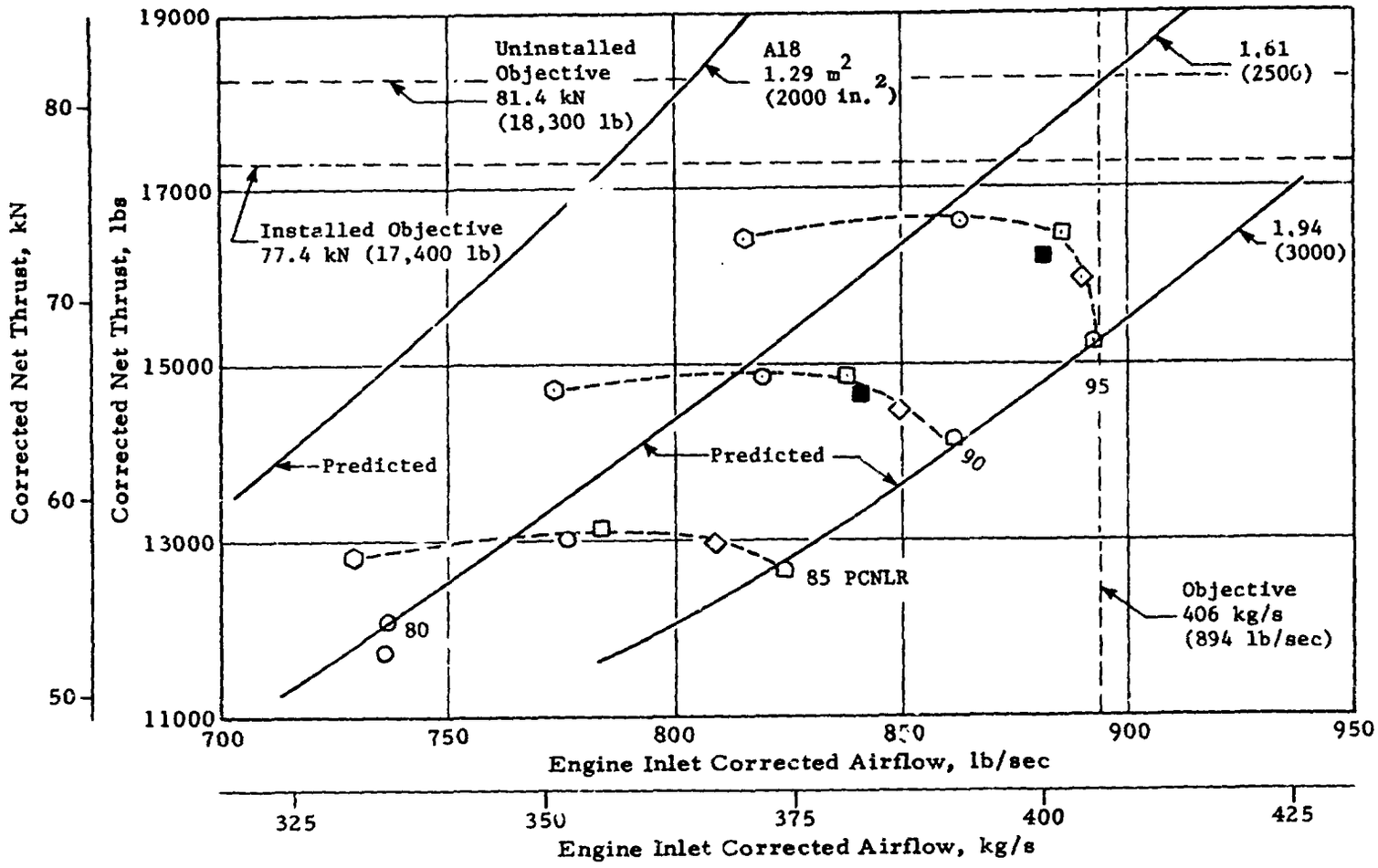

Figure 3. Thrust Versus Airflow, 0° ROPDEG.

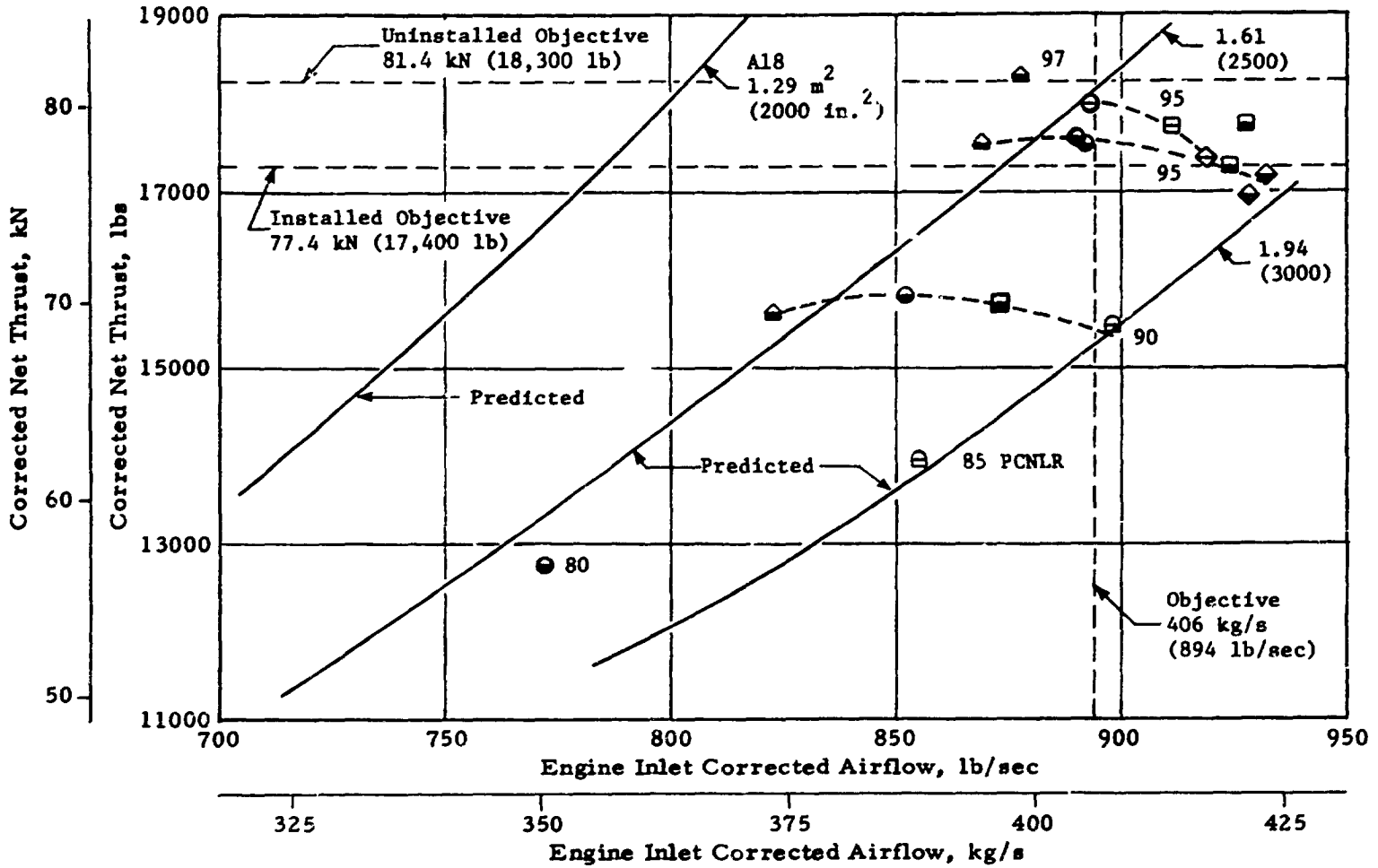

Figure 4. Thrust Versus Airflow, -3° ROPDEG.

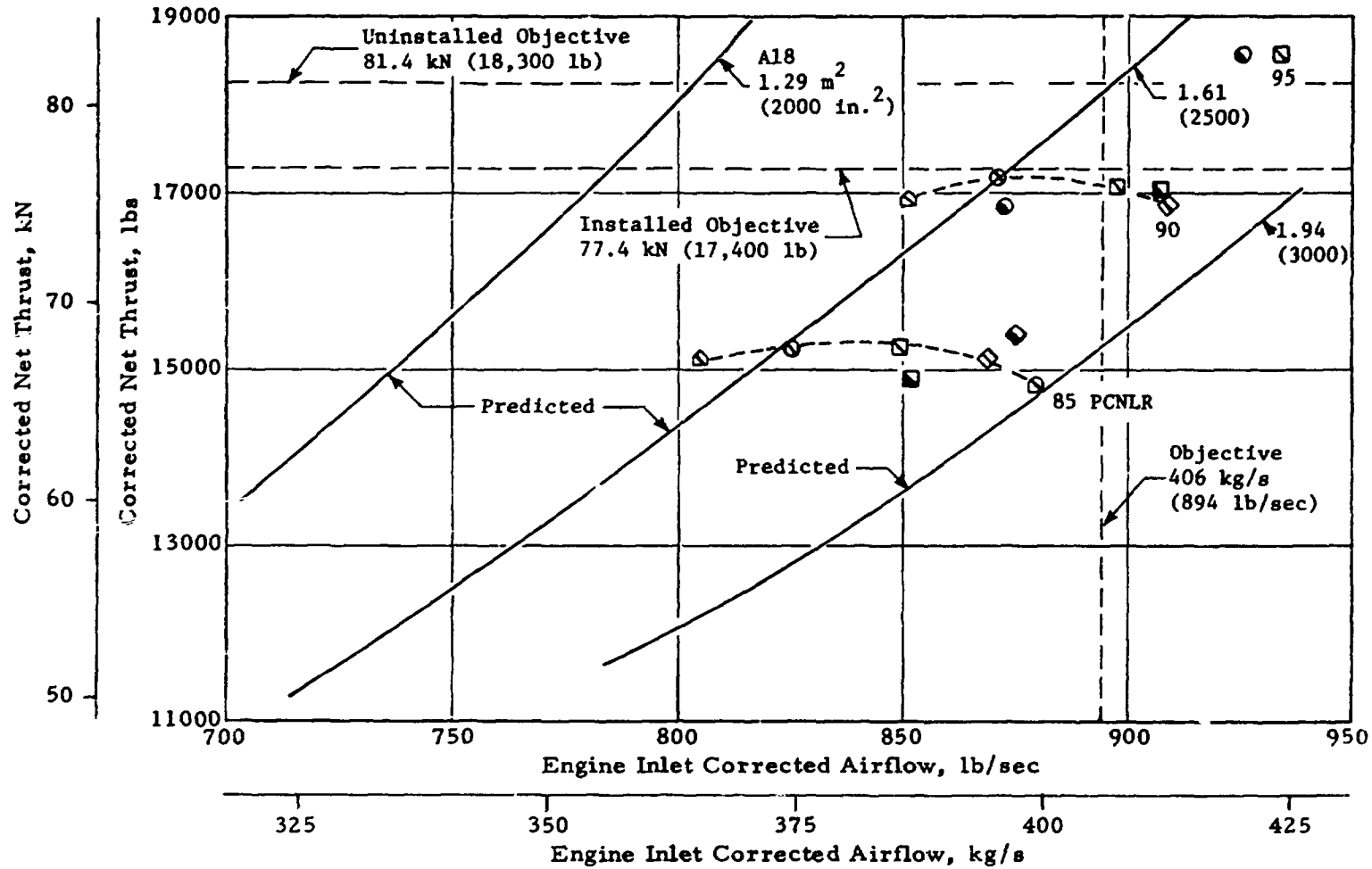

Figure 5. Thrust Versus Airflow, -5° ROPDEG.

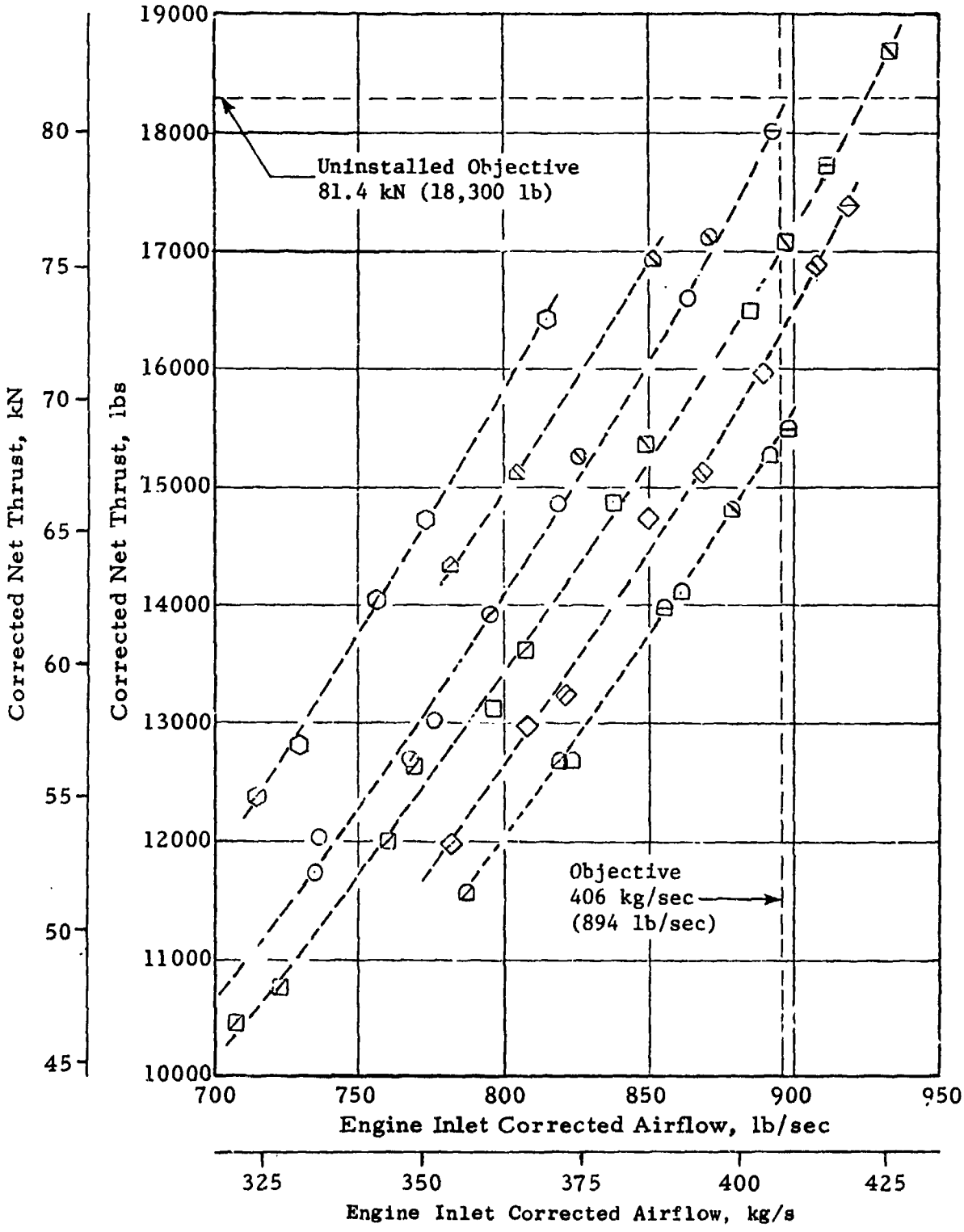

Figure 6. Thrust Versus Airflow with Bellmouth.

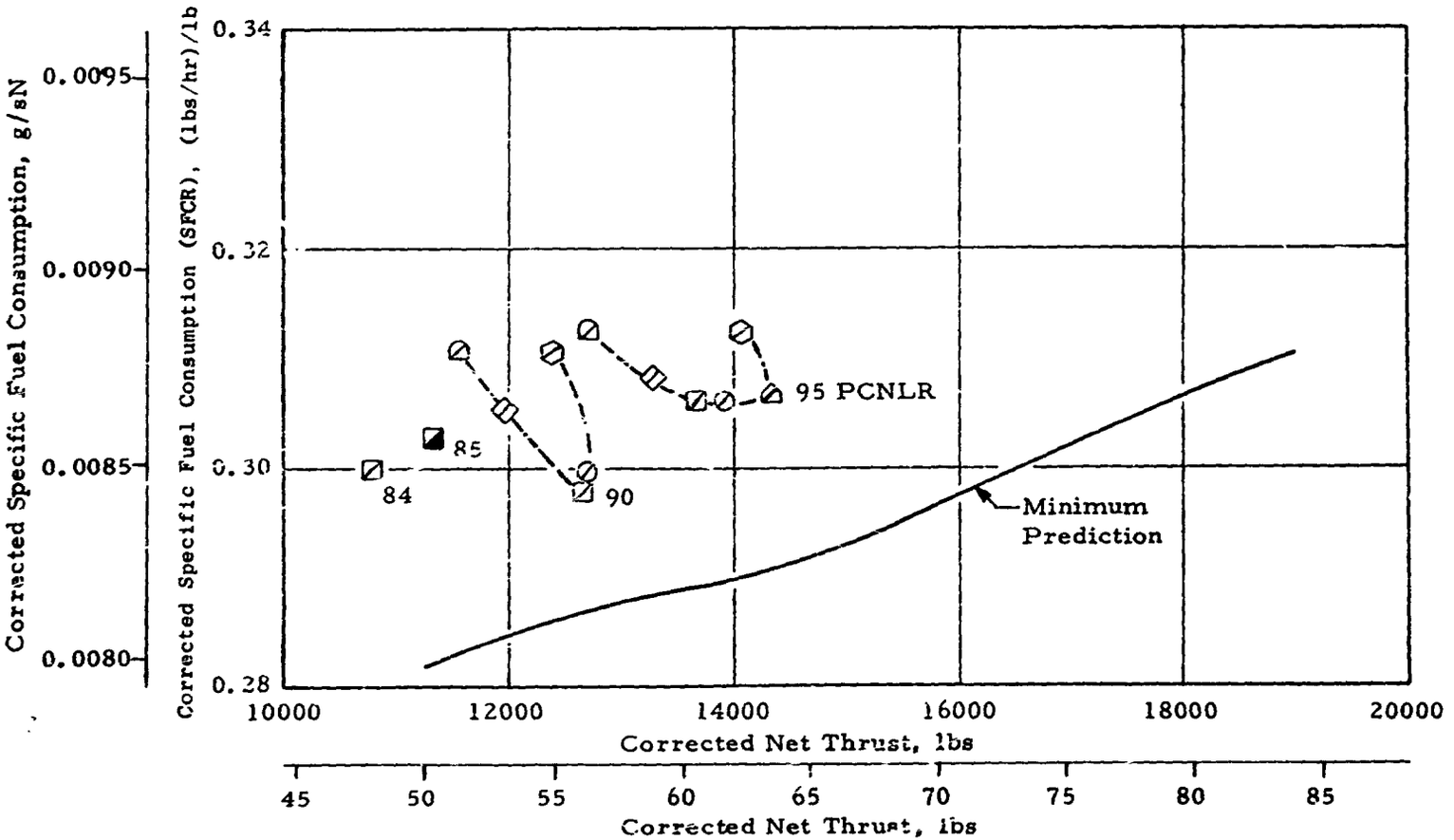

Figure 7. Specific Fuel Consumption Versus Thrust, +5° ROPDEG.

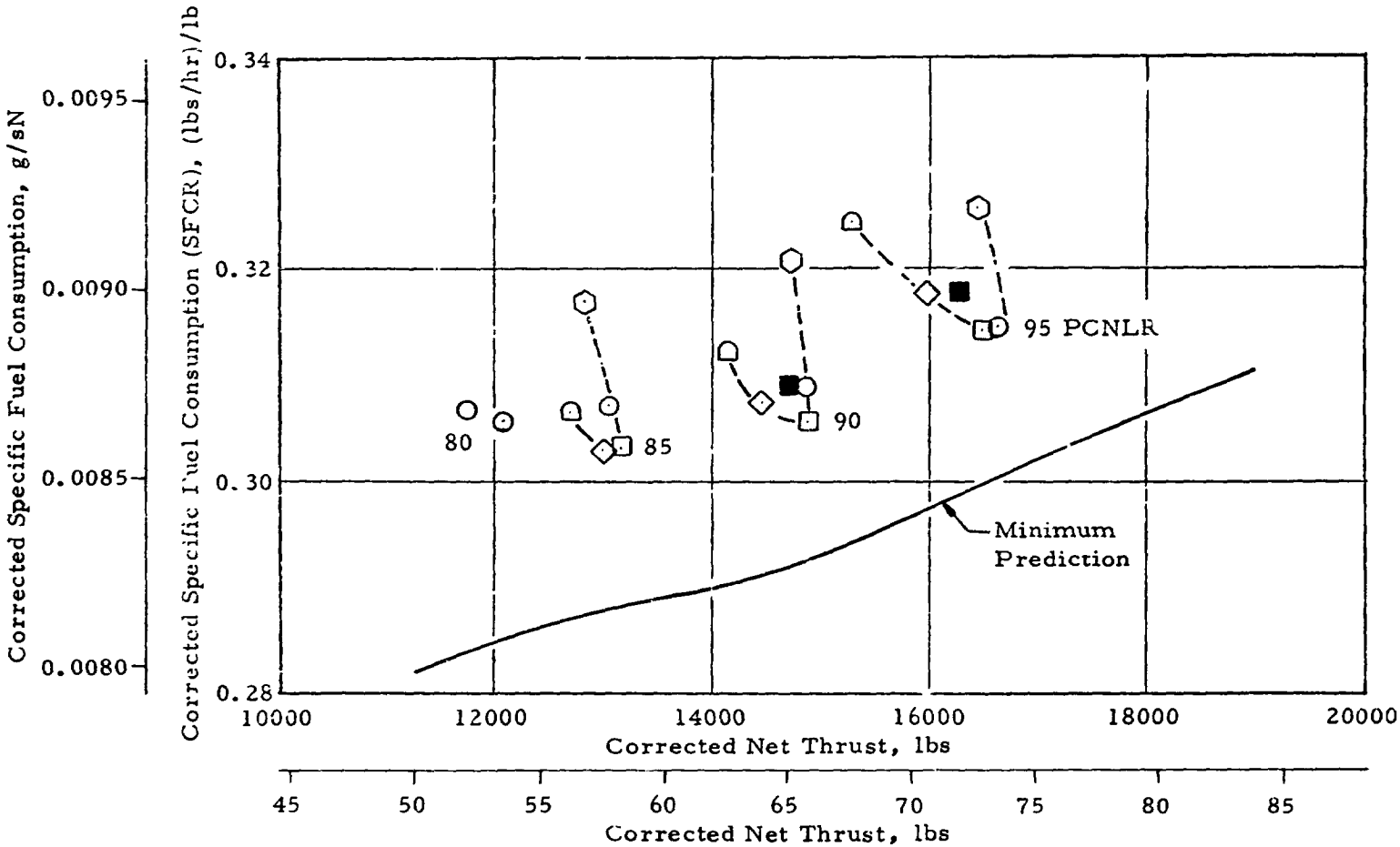

Figure 8. Specific Fuel Consumption Versus Thrust, 0° ROPDEG.

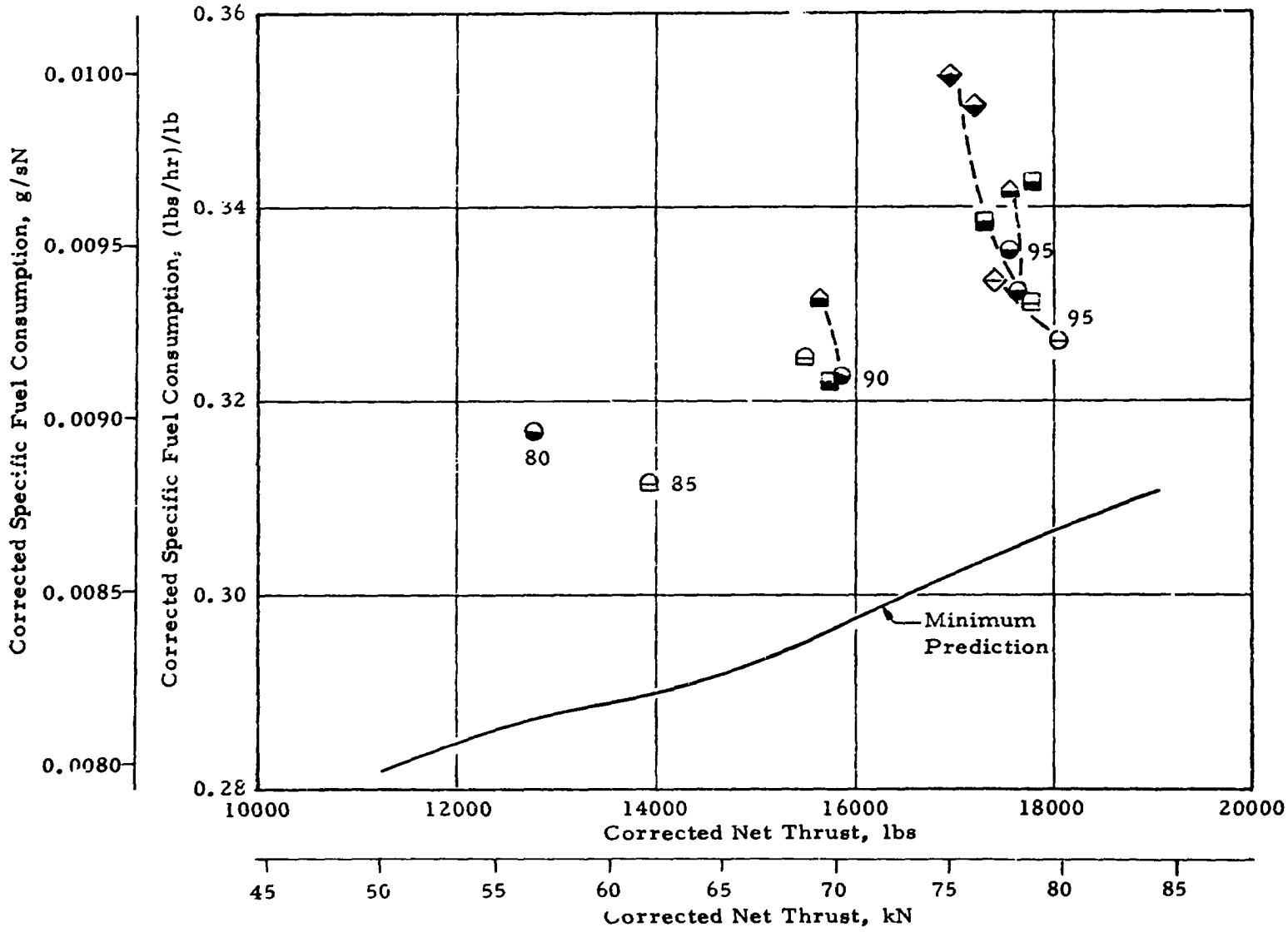

Figure 9. Specific Fuel Consumption Versus Thrust, -3° ROPDEG.

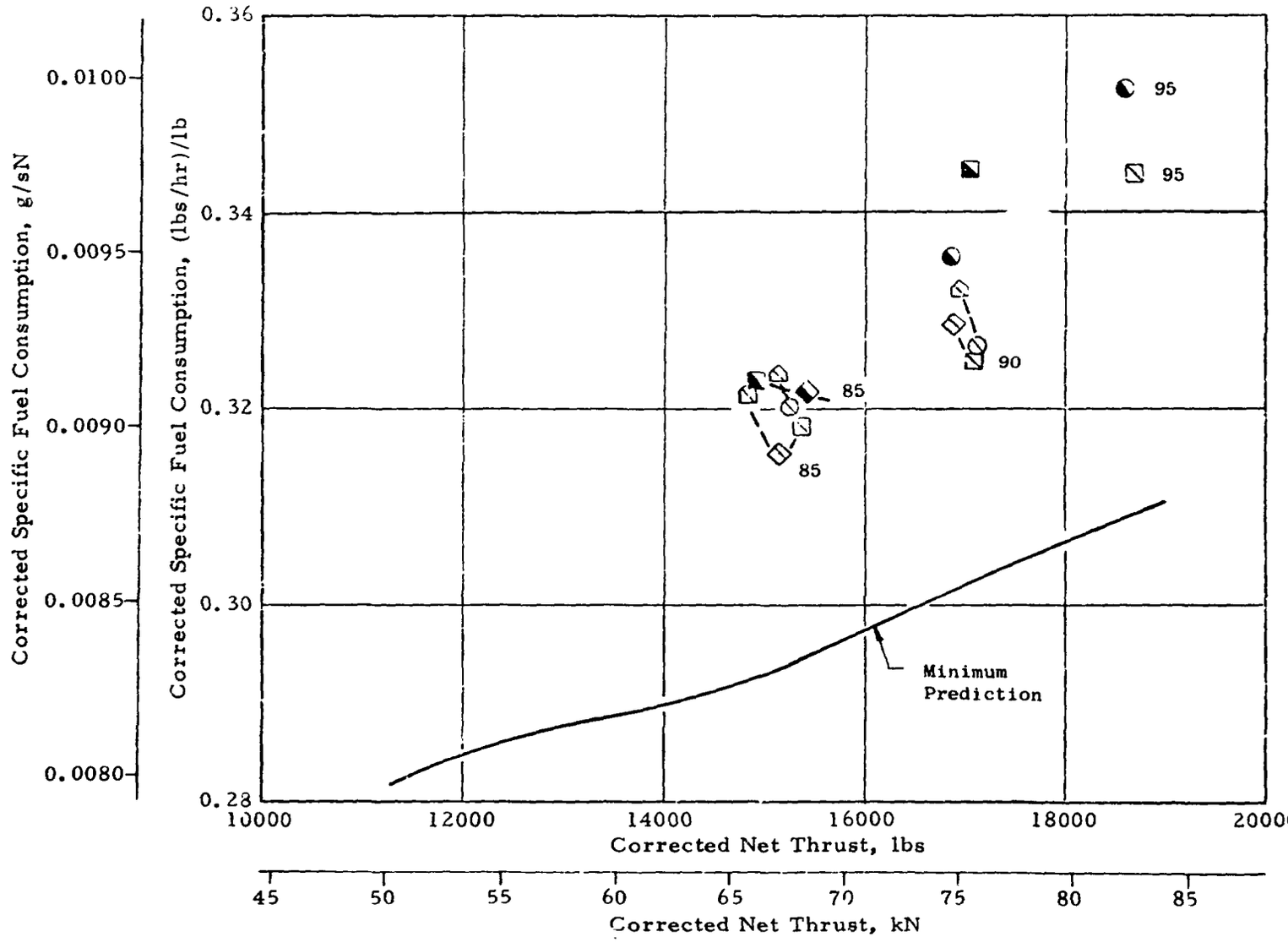

Figure 10. Specific Fuel Consumption Versus Thrust, -5° ROPDEG.

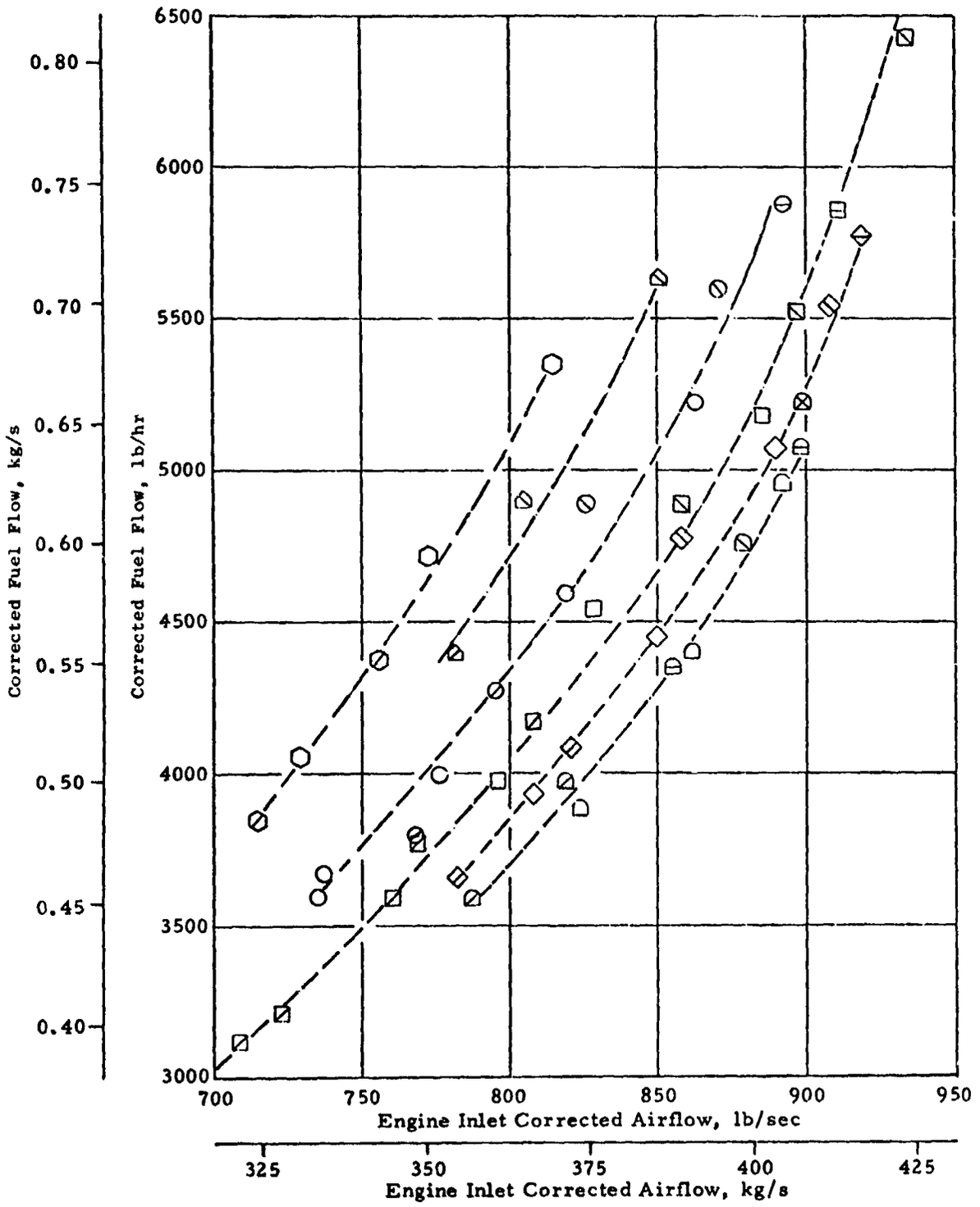

Figure 11. Fuel Flow Versus Airflow with Bellmouth.

3.3 INSTALLED PERFORMANCE

The installed thrust objective was 77.4 kN (17,400 lb). There were no sfc or turbine temperature objectives installed. At this thrust level, turbine inlet temperature was 4 K (8° F) lower than the uninstalled value. The installed performance included the ram recovery effects of the aero-acoustic inlet and some minor drag terms associated with the pylon and exhaust cowls.

The values shown in Table 1 for the experimental engine are based on scaling a test point at comparable installed thrust at Peebles ambient conditions to a 311 K (90° F) day at sea level, and adjusting thrust for 133 N (30 lb) loss associated with the pylon and exhaust cowl drag. The fan pitch angle was -2.9° for this point.

3.3.1 Thrust Versus Airflow

Thrust airflow data with the high Mach inlet installed also are included in Figures 2 through 5. Only a few installed data points are available for direct comparison with corresponding bellmouth points. In Figure 3 (0° ROPDEG), the points at 1.61 m^2 (2500 $in.^2$) indicated area are about 1.5% lower in thrust, as expected. In Figures 4 and 5, some of the installed points are higher in thrust than the corresponding uninstalled data, but this should be due to blustery ambient conditions affecting the quality of the installed data.

Thrust-airflow characteristics for all the installed data are shown in Figure 12. At takeoff airflow and exhaust area, the installed thrust is about 2% lower than the uninstalled values shown in Figure 6. Increasing indicated nozzle area above 1.87 m^2 (2900 $in.^2$) did not affect engine performance. At large areas, the flaps were diverged so far that the flow no longer stayed attached; the nozzle throat probably was set at the hinge-line area.

3.3.2 Specific Fuel Consumption

The variation of installed specific fuel consumption with thrust is included in Figures 7 through 10. As expected, where points are comparable to uninstalled data, the installed sfc is higher. Comparison of specific trends is difficult from the available data, however, because of data scatter. The fuel flow trends for all the installed data are shown in Figure 13. At lower airflows, the fuel flow tends to be higher than that of the bellmouth data. At higher airflows, the fuel flow is comparable to uninstalled levels, but data quality may be a factor here.

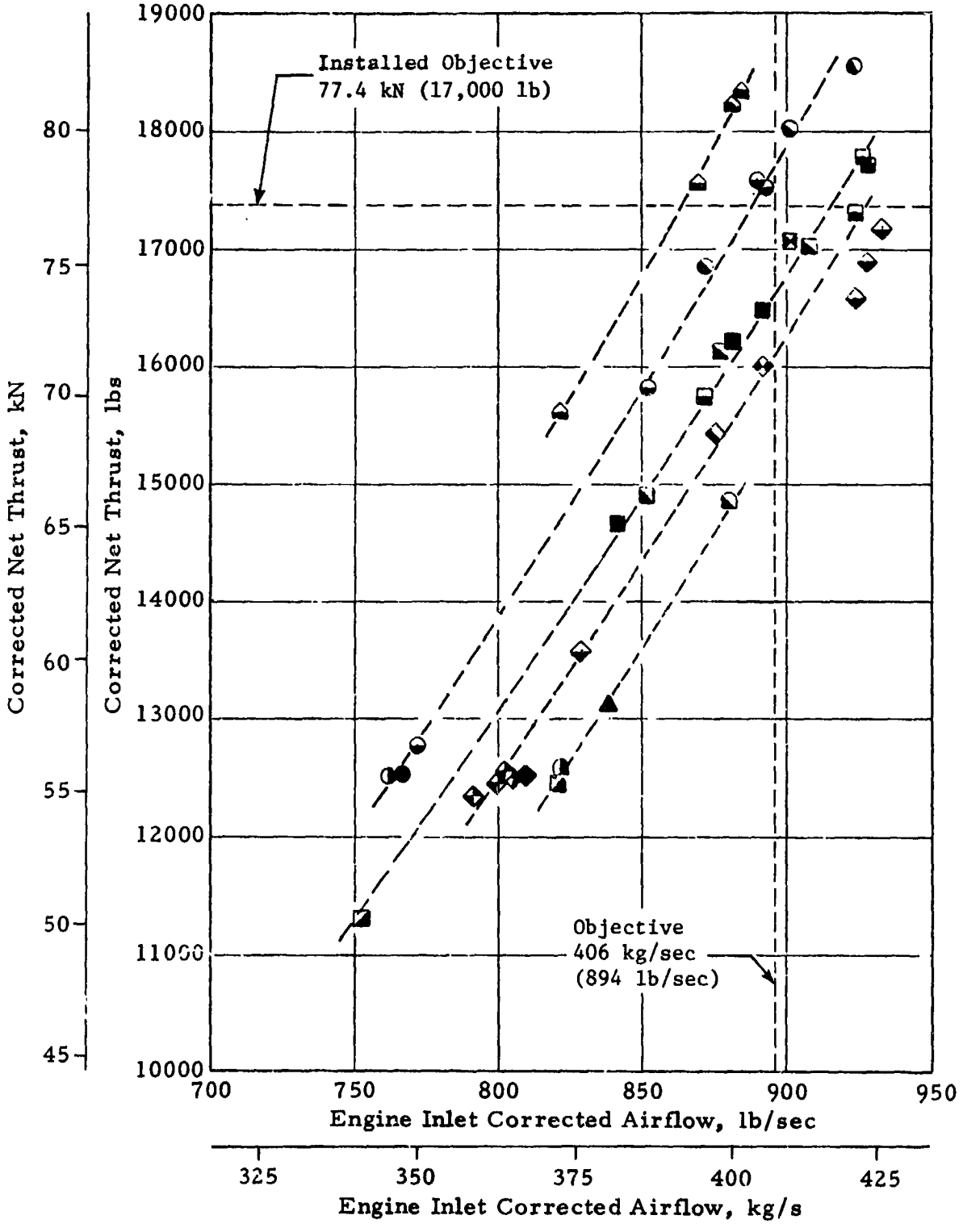

Figure 12. Thrust Versus Airflow, Installed.

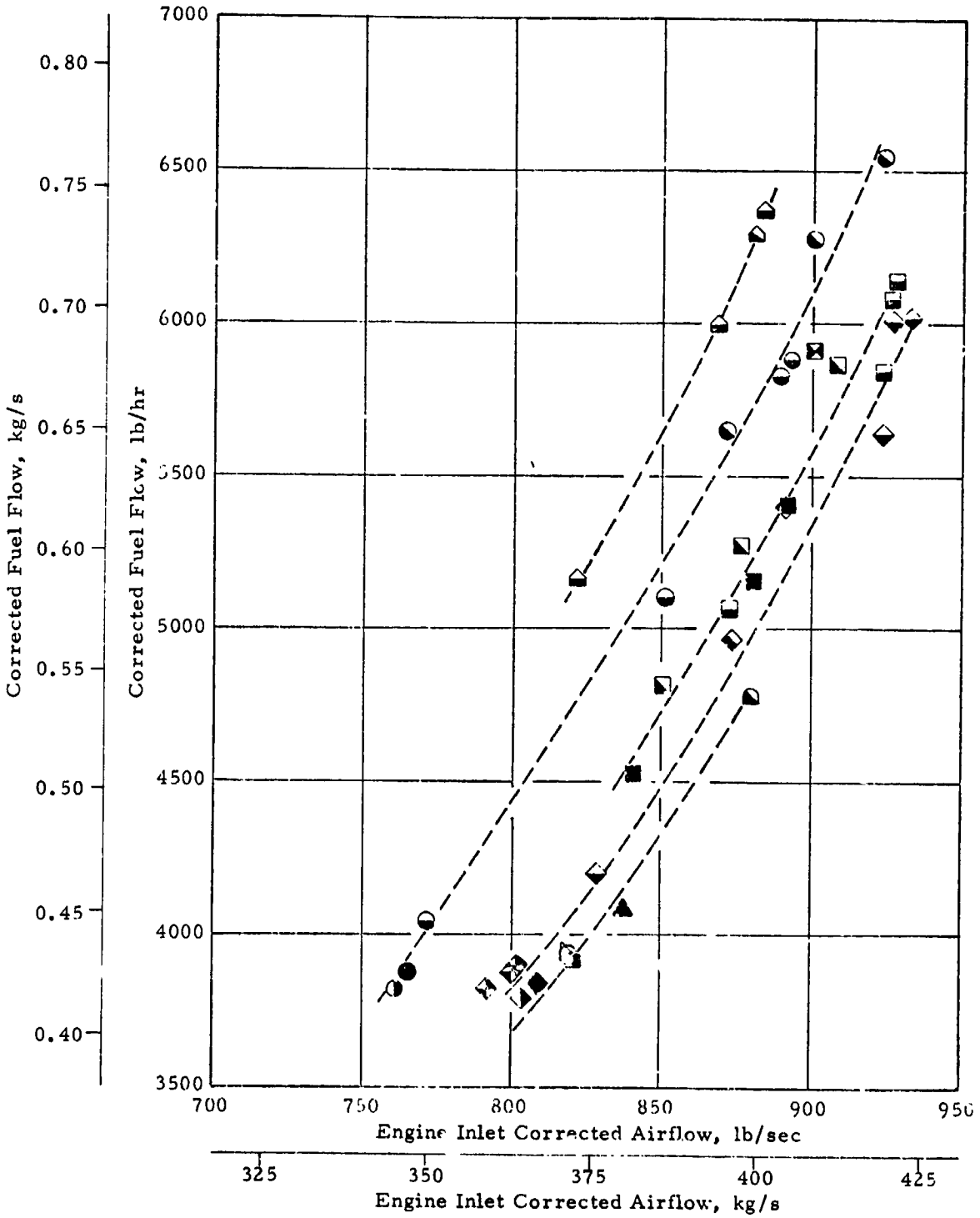

Figure 13. Fuel Flow Versus Airflow, Installed.

3.4 EXHAUST VELOCITY

The bypass exhaust stream and core exhaust stream velocities are shown in Figures 14 and 15, respectively, for the installed data readings. The bypass exhaust velocity at installed takeoff thrust is about 197 m/s (645 ft/sec). The core stream velocity is about 256 m/s (840 ft/sec).

3.5 REVERSE THRUST MODE

The reverse thrust objective was 35% of takeoff thrust. The original program plan called for demonstration of reverse thrust by fan blade rotation through either flat pitch or stall pitch. However, the test results obtained from the 50.8-cm (20-in.) model fan showed that the desired thrust level could not be obtained by rotation through flat pitch because of the high fan speed required. Also, due to the reverse blade camber in this mode, the noise goal would have been exceeded. Consequently, it was decided to reverse only through stall during the engine test.

In the stall pitch direction, it was expected that objective reverse thrust would be achieved at -95° fan pitch angle, at 185 kg/s (408 lbs/sec) airflow. This operating condition was not demonstrated because of the nozzle flap support ring failure.

The flowpath for reverse mode operation is shown in Figure 16. In this mode the exlet flaps were positioned to maximum divergence. The inlet rakes were reversed. The fan discharge and turbine discharge rakes were removed because acoustic tests had also been included as part of the scheduled test. Airflow was based on the static pressure measurements from taps on the inner and outer duct wall aft of the fan stator. The splitter was installed for the first time during the engine test.

Only five readings were taken in reverse mode, three of which could be reduced with reasonably valid results. Only minimal instrumentation was operational since the engine was in an acoustic configuration. The estimated airflow was close to the predicted level based on performance of the 50.8-cm (20-in.) simulator; however, fan exhaust pressure ratio was low.

The test data are shown in Figure 17 along with predicted trends for the two pitch angles which were run. The test data indicate that the objective thrust of 27.1 kN (6090 lb) probably would not have been achieved, even if the desired operating conditions were run. Possible reasons for these low performance levels are discussed in Section 4.0.

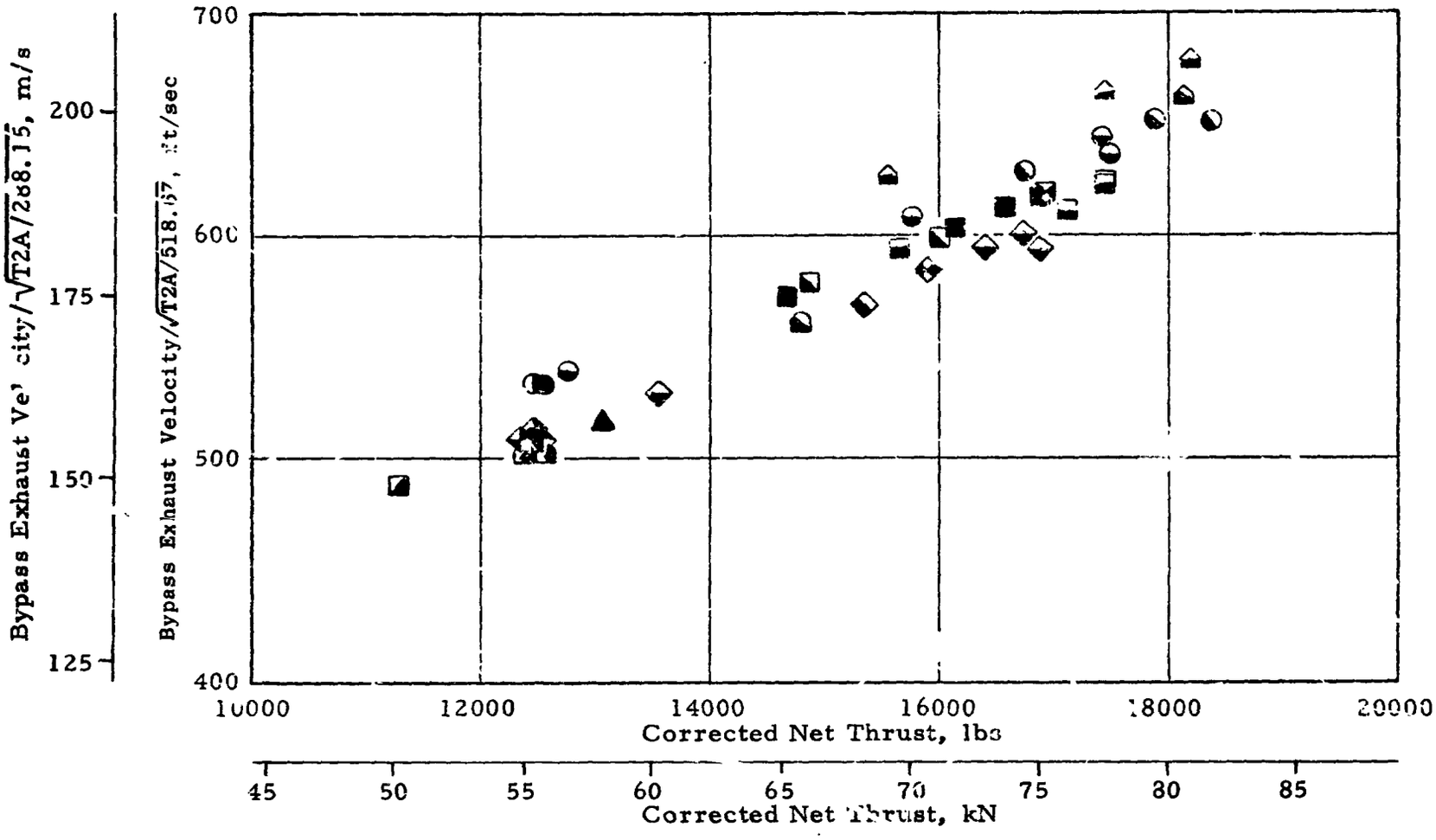

Figure 14. Bypass Exhaust Velocity Versus Thrust.

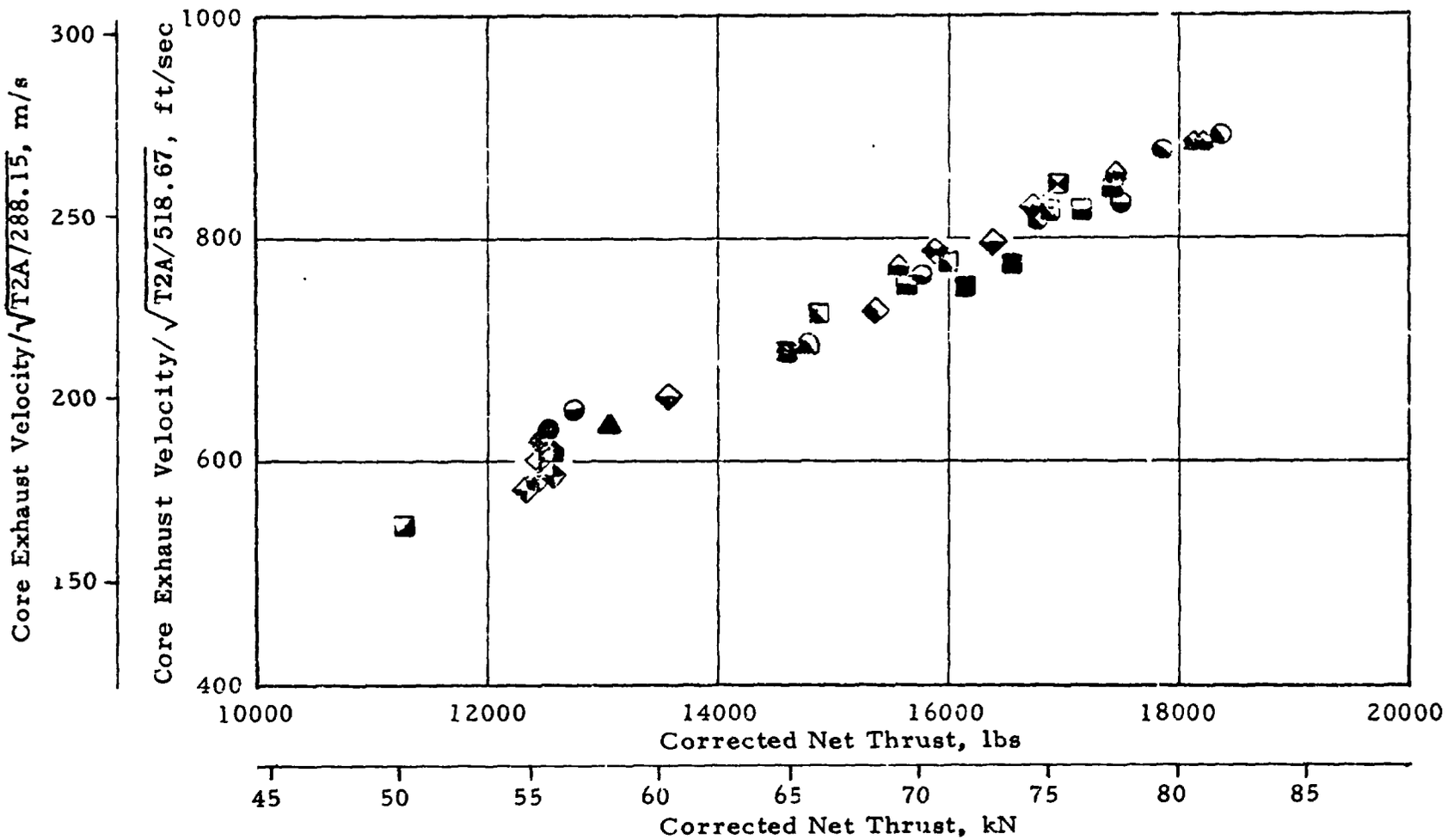

Figure 15. Core Exhaust Velocity Versus Thrust.

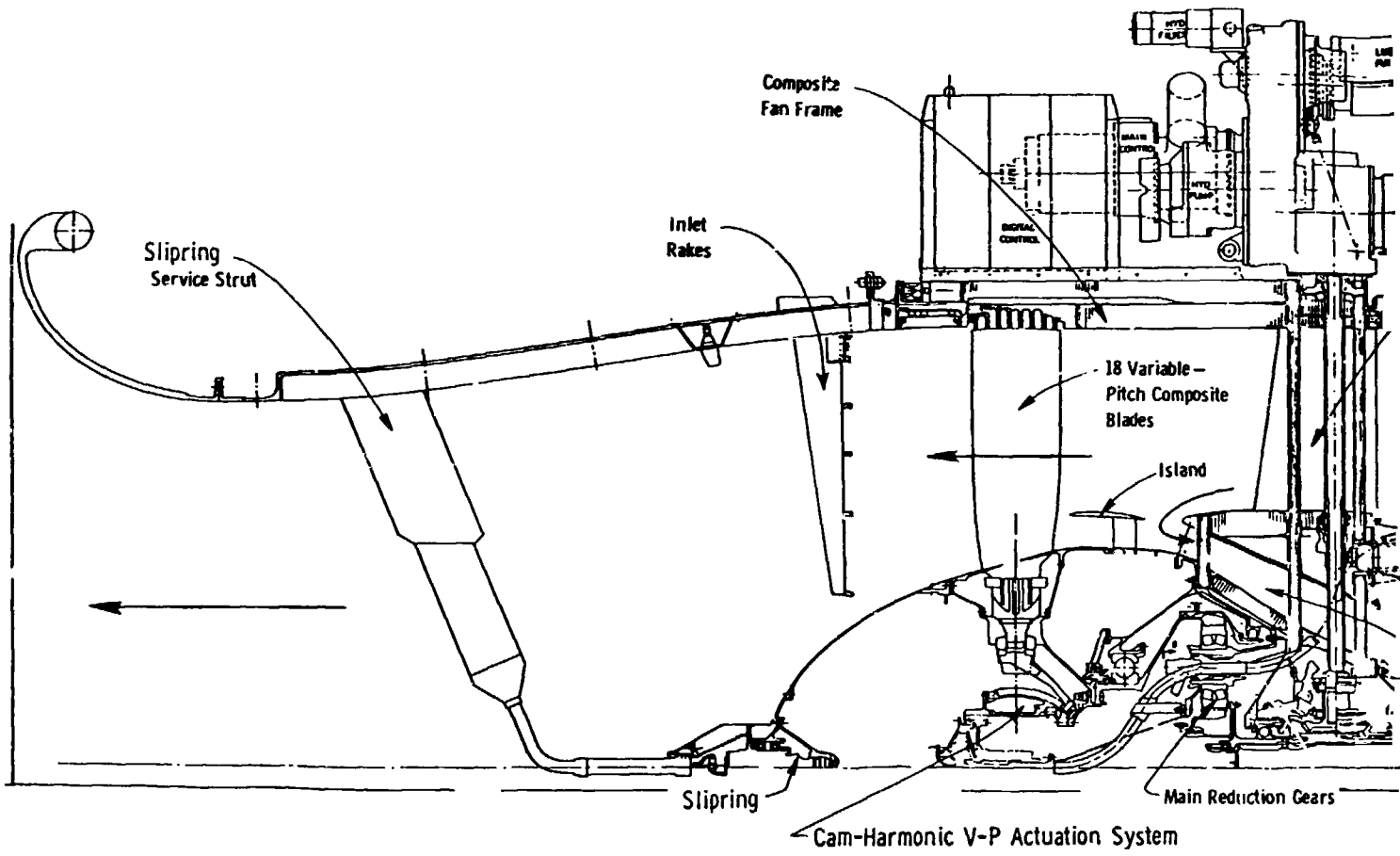

Figure 16. UTW Propulsion System Cr

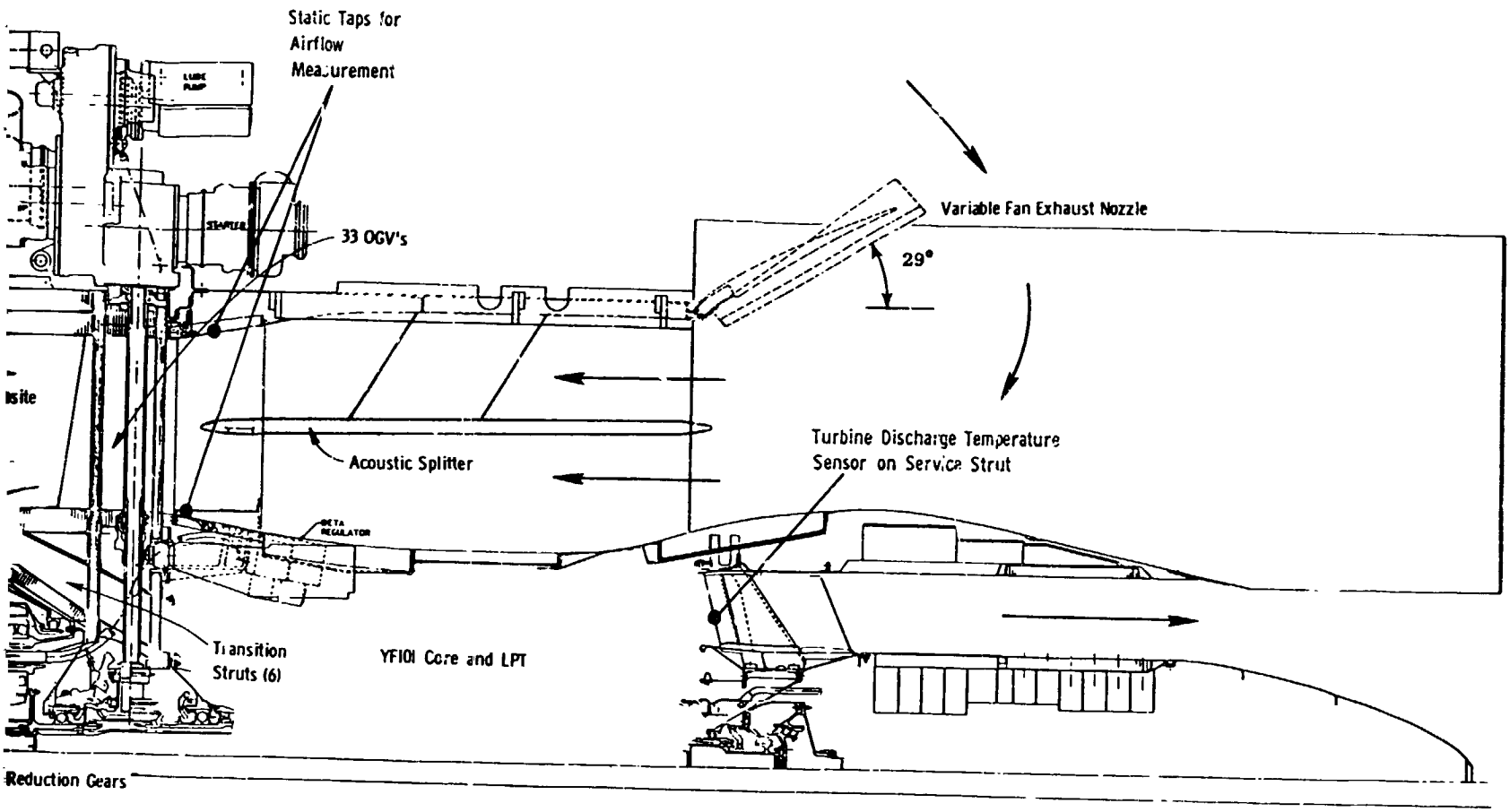

.on System Cross Section Showing Reverse Mode Flow Direction.

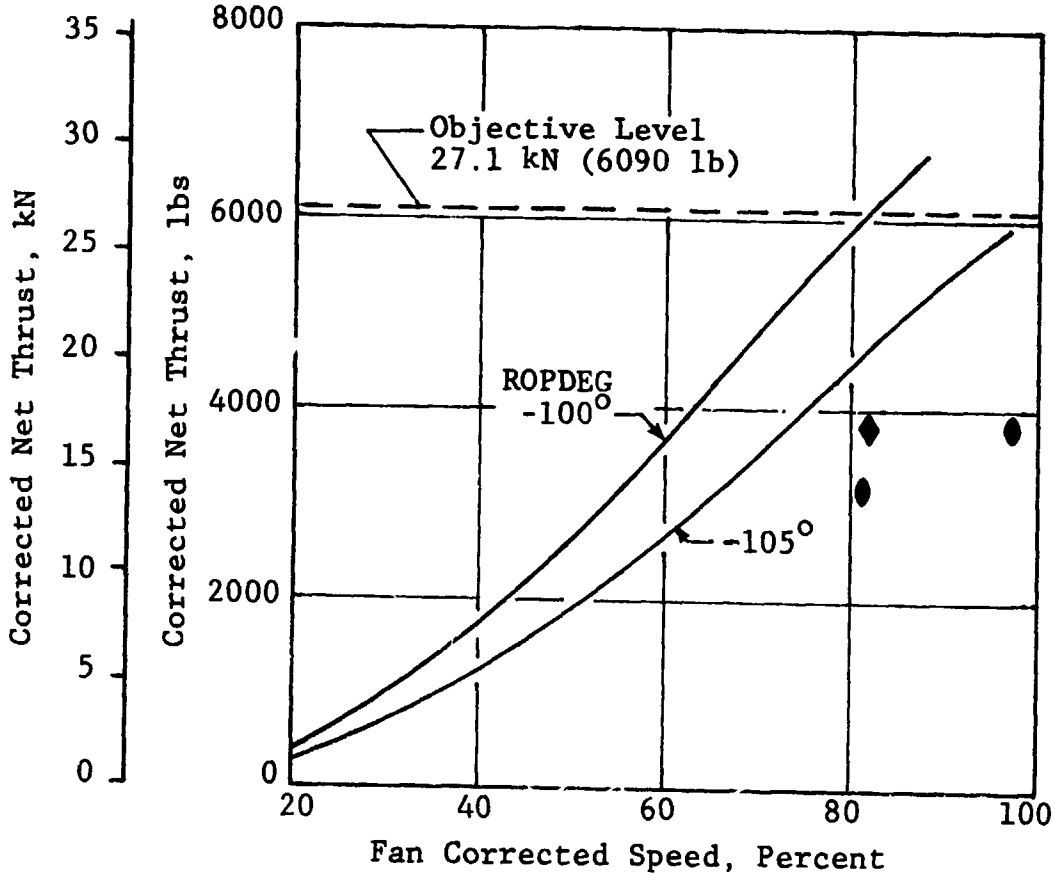

Figure 17. Thrust Versus Fan Speed, Reverse Mode.

Plotting Symbols.

Indicated Bypass Exhaust Nozzle Area		Fan Pitch Angle (ROPDEG) Bellmouth		Inlet
⬡ 1.36 m^2	(2100 in^2)	⊕	7°	◕
⌂ 1.45	(2250)	⊘	5°	◕
○ 1.52	(2350)	◐	3°	◑
□ 1.61	(2500)	○	0°	●
◇ 1.71	(2650)	⊖	-3°	◒
△ 1.81	(2800)	⊘	-5°	◔
⌂ 1.87	(2900)	⊗	-7°	◓
◺ 1.90	(2950)			
◺ 2.00	(3100)			

Reverse Mode Fan Pitch Angle (ROPDEG)

- ⬮ -105°
- ⧫ -100°

4.0 UTW FAN AERODYNAMIC PERFORMANCE

4.1 FORWARD MODE

4.1.1 Fan Aero Design and Scale Model Test

Details of the QCSEE under-the-wing (UTW) fan design, both aerodynamic and mechanical, are given in References 1 and 2. Briefly summarizing, the aerodynamic design point for the UTW fan was selected midway between takeoff and altitude cruise engine operating conditions. Design-point corrected tip speed was 306 m/sec (1005 ft/sec) with an average fan bypass pressure ratio of 1.34 and an average fan core pressure ratio of 1.23. Design-point bypass ratio was 11.3 and the objective adiabatic efficiencies were 88.0% for the bypass portion and 78.0% for the core portion.

An exact linear scale model of the fan component (scale factor of 20÷71) was tested in the Aero/Acoustic Facility at the GE Research and Development Center in Schenectady, New York prior to UTW engine tests. Facility constraints required a modification to this Simulator Fan in the bypass duct and the transition (or core inlet) duct, but the geometry of the engine's fan rotor and OGV's were accurately modeled. The fan performance of the Simulator was evaluated for both forward-thrust and reverse-thrust modes, with both bellmouth and high Mach inlets, along several operating lines at three rotor blade pitch angle settings. Details of the test results are given in Reference 3. Although the Simulator did not achieve its design-point flow and pressure ratio objectives at the design rotor pitch angle, it was recognized that the variability of both the rotor blades and the bypass-stream exhaust nozzle in the engine would allow specific operating-point objectives to be attained with the original design.

Following the scale model tests, the fan overall-performance representation in the UTW engine-cycle deck was revised by curve-fitting the Simulator data. The cycle deck's fan pressure ratio versus flow and speed relationships were adjusted using the test data, and the efficiencies generally were within a point of the measured data. Details of this revised performance representation, upon which the estimates of the UTW-engine fan performance were based, are given in Reference 2. During tests of the engine, the fan's overall performance was then compared to the cycle deck's predicted levels.

4.1.2 Fan Bypass Region Overall Performance

Performance characteristics of the engine fan bypass region are presented in Figures 18 through 20 for tests with the bellmouth inlet installed. Measured test data, through which solid lines are drawn, are plotted against background dashed lines which correspond to the revised-fan-performance representation discussed in Section 4.1.1. Data were taken primarily in the unthrottled region, well below the estimated fan stall line. However, sufficient data were obtained to demonstrate objective performance in the

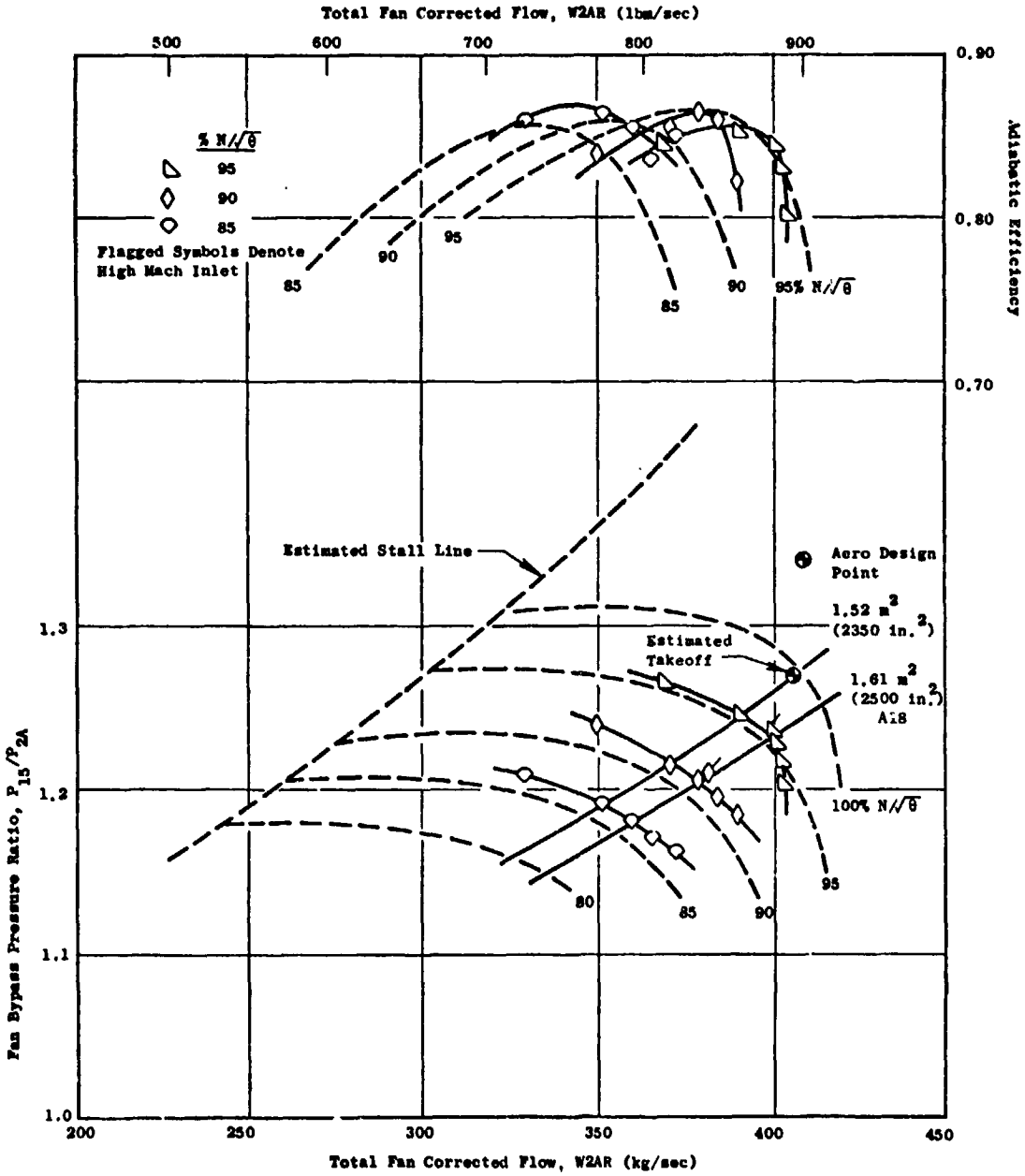

Figure 18. QCSEE UTW Engine Fan Bypass Performance at β_F = 0° (Nominal) Rotor Pitch Setting with Inlet Bellmouth.

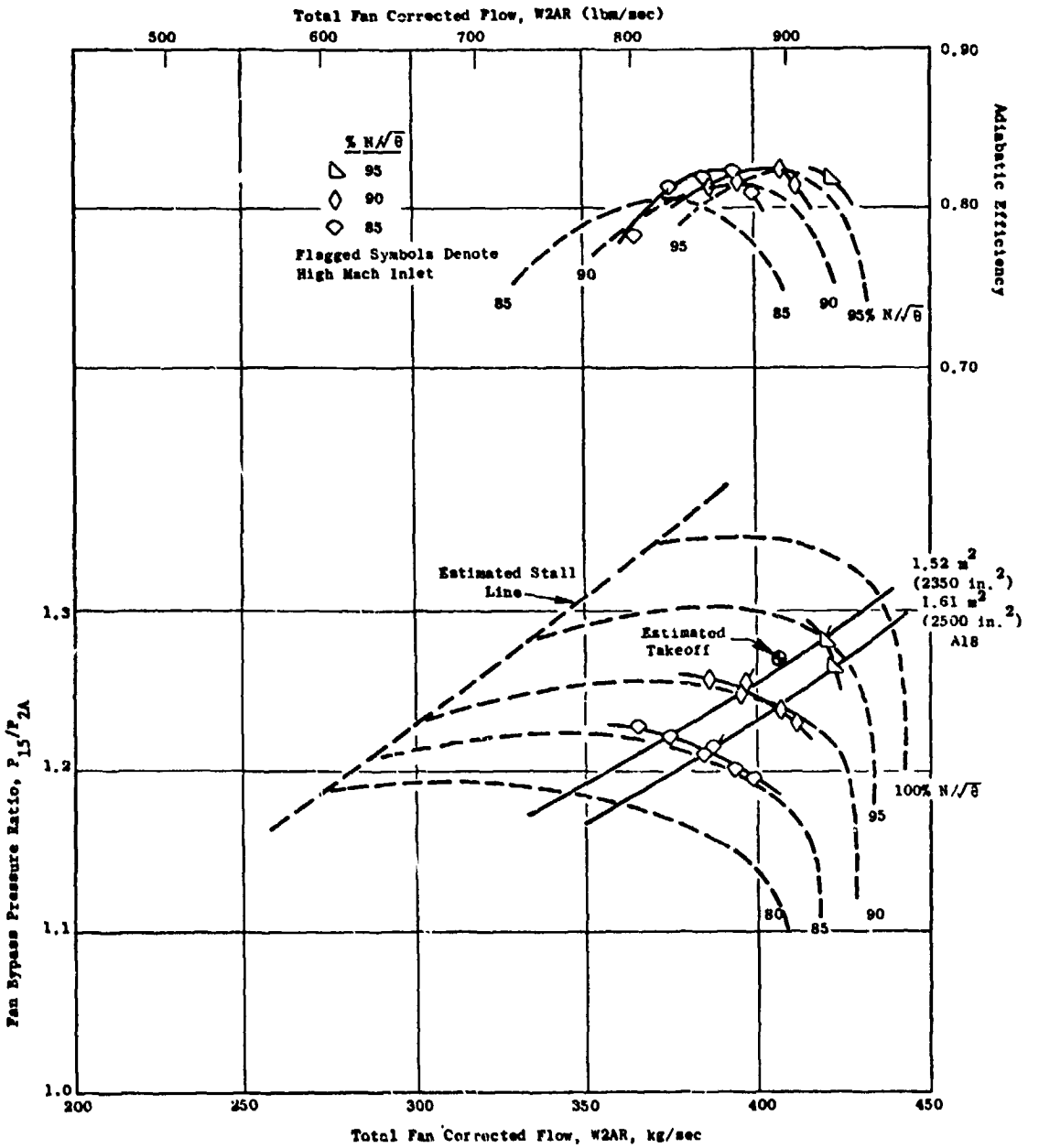

Figure 19. QCSEE UTW Engine Fan Bypass Performance at β_F = -5° (Open) Rotor Pitch Setting.

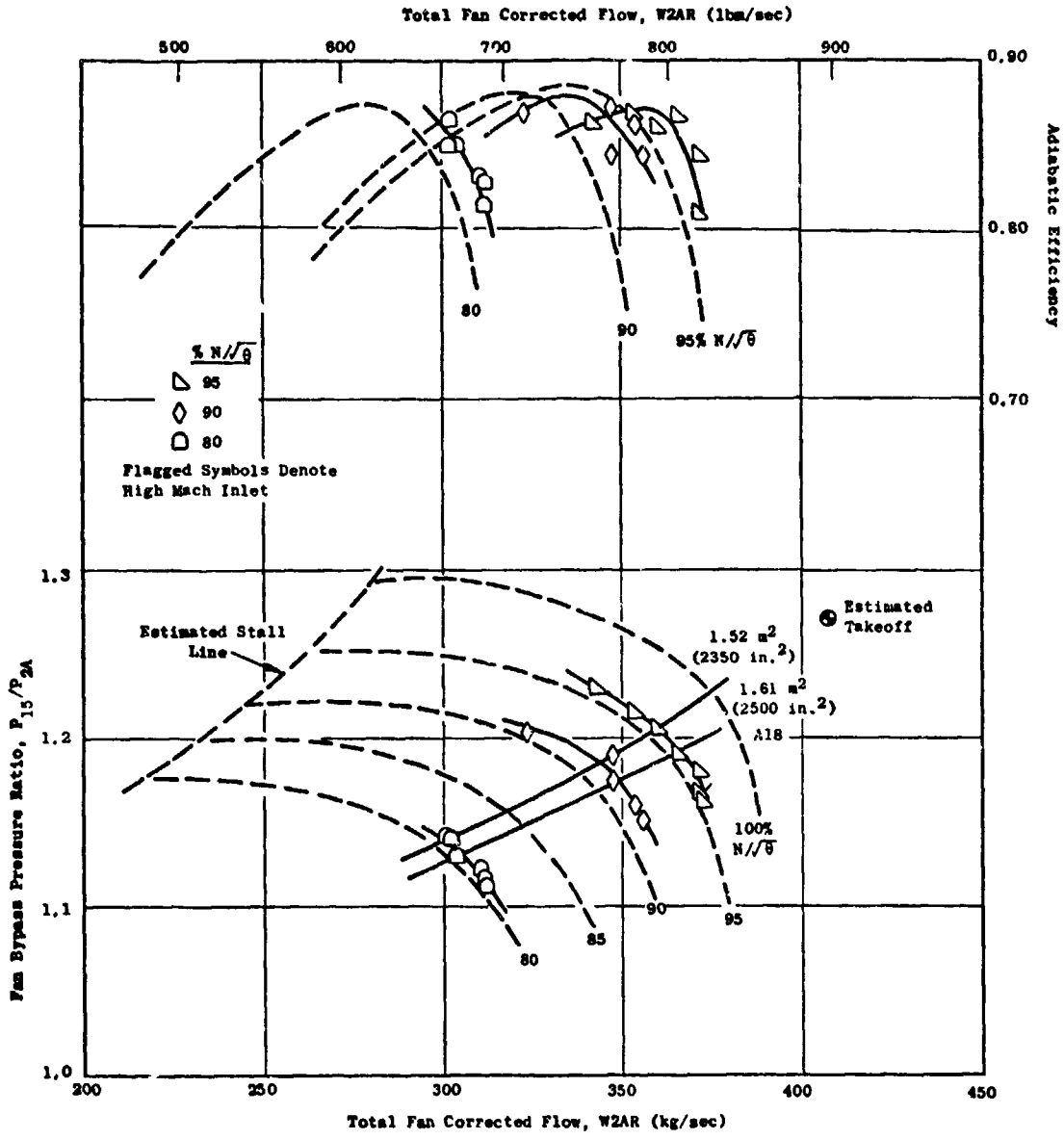

Figure 20. QCSEE UTW Engine Fan Bypass Performance at β_F = +5° (Closed) Rotor Pitch Setting.

vicinity of the expected takeoff operating condition and to establish the level of fan peak efficiency over the high-speed range. Fan performance at all speeds and blade pitch settings tested showed good agreement with the cycle deck representation. Fan efficiency in the unthrottled region is equal to or slightly greater than the estimated values in the cycle representation, and peak efficiencies agree with predicted values within a point at each speed tested. Over the low-speed range tested, the fan pumping capacity slightly exceeded the predicted values of flow by 1% - 2% along operating lines near peak fan efficiency. Figures 18 through 20 show this trend to be consistent at all rotor pitch settings tested, and indicate that these discrepancies decreased as the blade was opened. These differences between measured and predicted flows also decreased as the fan speed increased at a given blade pitch setting. At the highest speed tested with the bellmouth inlet (95% of design speed), the measured flow was less than 1% higher than predicted.

As was seen in the scale model tests, no significant differences in the pumping capability of the fan were observed between data taken with the bellmouth inlet and with the high Mach inlet. Data points of direct comparison are shown in Figures 18 through 20; those taken with the high Mach inlet are denoted with a flagged symbol. The fan inlet pressure was accurately determined by considering the boundary-layer rake-pressure measurements, and flow was determined from analytical correlations of scale-model inlet data. In the relatively unthrottled region of operation, there was no apparent effect on the fan rotor caused by the thickened rotor-tip-inlet boundary layer, and the data indicated no significant shifts in either constant speed lines or lines of constant nozzle area on the performance map. A comparison of fan efficiency between the bellmouth and high Mach inlet data was not as straightforward since the data reduction procedure and the available instrumentation could not account for any boundary-layer profile effects at the fan discharge as was done in the inlet. Higher fan efficiencies were calculated from the high Mach inlet data than from the bellmouth data, but are not shown in Figures 18 through 20 since the comparison would not be valid. A fairer "weighting" technique for the fan discharge conditions would have lowered the calculated efficiencies toward the values achieved during the bellmouth testing.

4.1.3 Fan Hub (Core Inlet) Region Overall Performance

Performance characteristics of the engine fan-hub region were measured by radial rakes located in the transition (core compressor inlet) duct and are presented in Figures 21 through 23. It was found to be more meaningful to correlate fan-hub pressure rise and efficiency against total fan flow rather than core flow, as the axial gap between the island trailing edge and the flow splitter leading edge tends to lessen the influence of core throttling on the fan. As in the bypass region, measured engine data, through which solid lines are drawn, are plotted against background dashed lines derived from the Simulator fan test results. Since little data were available from either the Simulator or engine fans to evaluate the efficiency of the fan itself separate from the loss characteristics of the transition

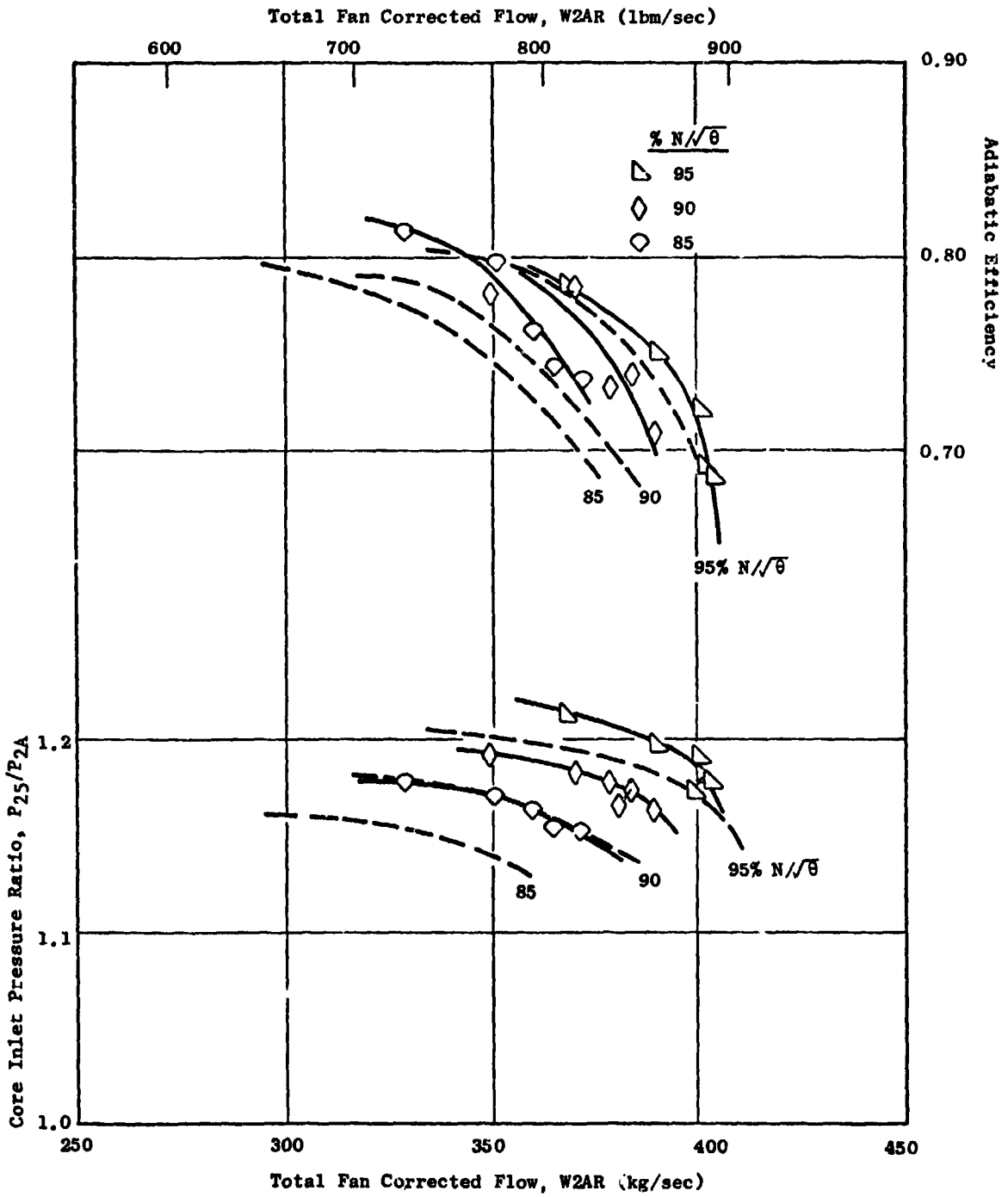

Figure 21. QCSEE UTW Engine Fan Hub Performance at β_F = 0° (Nominal) Rotor Pitch Setting.

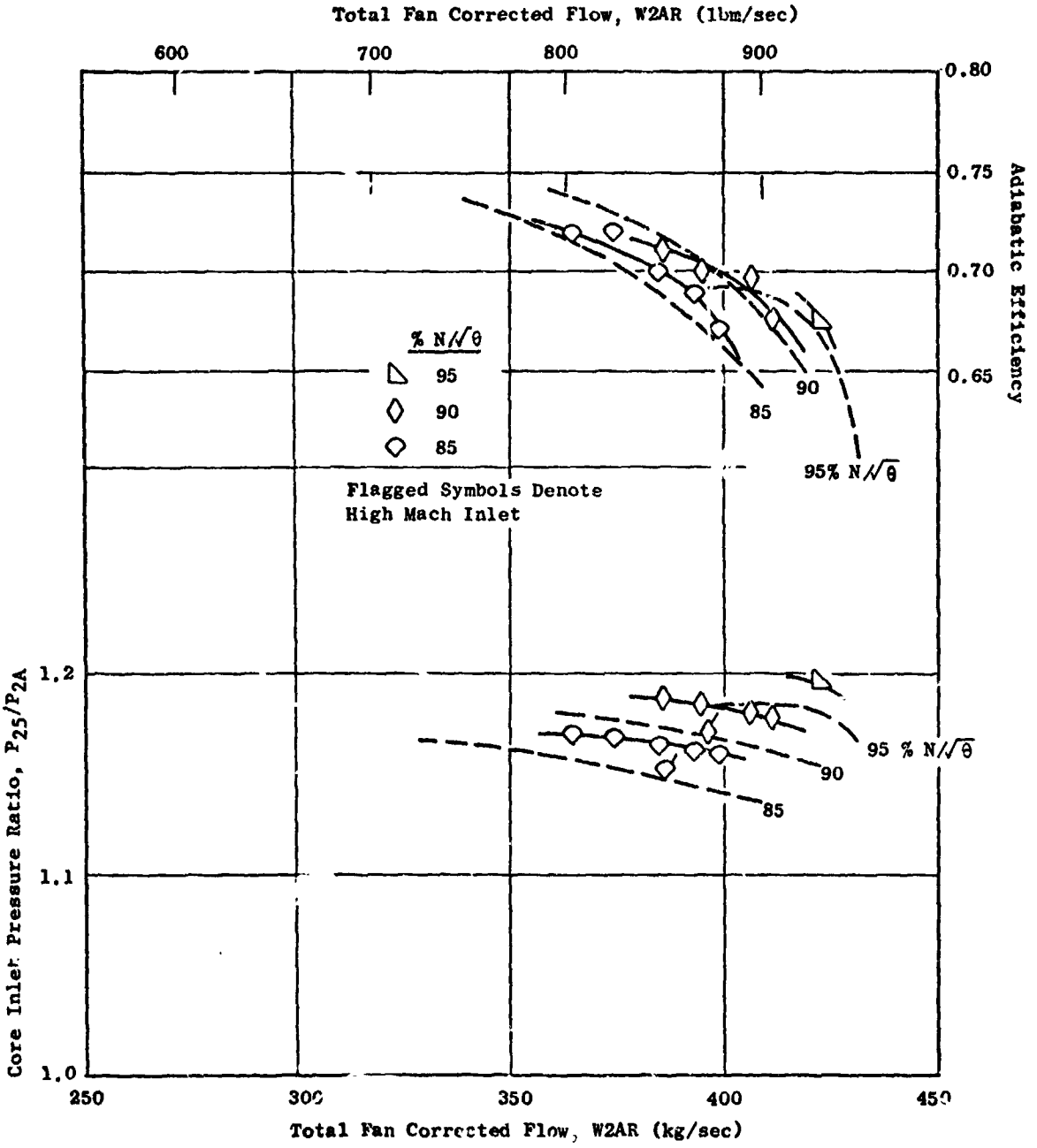

Figure 22. QCSEE UTW Engine Fan Hub Performance at $\beta_F = -5°$ (Open) Rotor Pitch Setting.

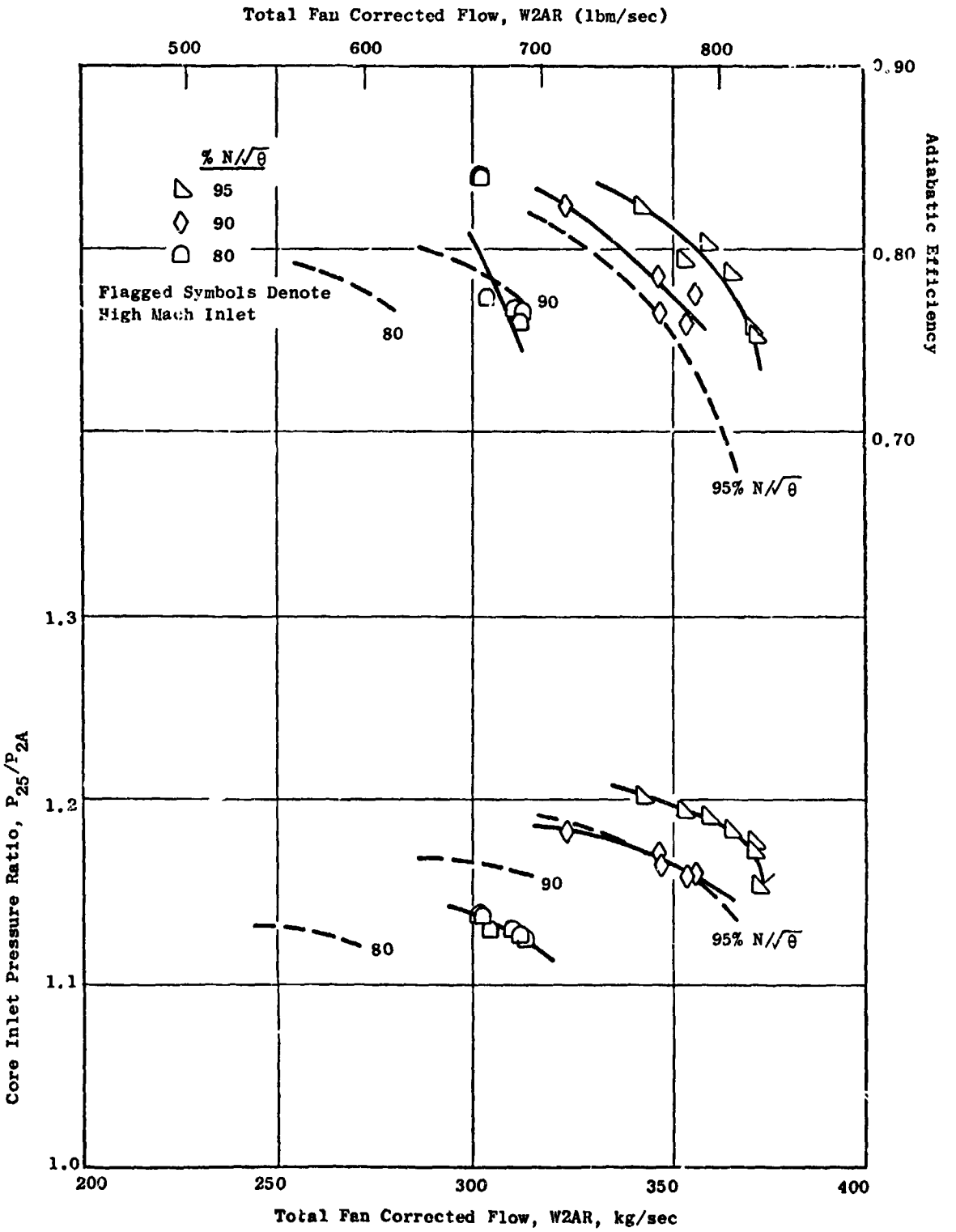

Figure 23. QCSEE UTW Engine Fan Hub Performance at β_F = +5° (Open) Rotor Pitch Setting.

duct, a comparison with Simulator data was made in Figures 21 through 23 of the measured performance determined by the core inlet rakes at Plane 25. Although slight differences existed between the engine and Simulator transition duct geometry and axial placement of the core inlet radial rakes, they were not considered significant enough to invalidate these comparisons.

Fan-hub performance generally exceeded that of the Simulator at all rotor pitch settings and speeds tested. Since the Simulator fan produced greater-than-design values of hub pressure ratio and adiabatic efficiency, the engine fan also demonstrated more-than-sufficient hub supercharging capability. The same overall trends in hub performance were observed in both the scale model and the engine as rotor pitch angle was changed. Efficiency increased along all speed lines as the fan was throttled and was highest for the +5° (closed) rotor pitch angle, decreasing as the rotor blade was opened toward the -5° (open) setting.

4.1.4 Rotor Exit Radial Profiles

Radial profiles of rotor-discharge and bypass-flow total pressure and temperature were defined by the data from the highest-reading elements on the arc/radial rakes in the bypass duct. Adiabatic efficiency was calculated from these data, and the results are shown in Figures 24 through 26 for a representative high speed, high efficiency point at each of the three blade angles tested. As was done in the overall-performance evaluation, comparison is made between the scale model test results and the engine data. Figures 24 through 26 show very similar profiles of rotor pressure rise and efficiency for the two fans, free of any localized depressions which would indicate trouble areas. There is a general tendency for the engine fan rotor to produce more pressure rise with better efficiency than the scale model in the tip region. These characteristics of the rotor profiles are exhibited at each of the three rotor pitch settings: 0° (nominal), +5° (closed), and -5° (open).

4.1.5 Bypass OGV Performance

Limited comparative data were available to allow a comparison between the scale model and the engine, since the majority of the Simulator data were taken with radial rakes positioned between OGV's rather than arc rakes. Of the three comparisons made in Figures 24 through 26, only the -5° (open) blade pitch setting of Figure 25 had sufficient data to determine complete stage efficiency profiles. This particular setting was observed to have the highest OGV loss level in the scale model tests, due to both off-design incidence angle and the high Mach number environment. As shown in Figure 25, the difference between rotor and stage efficiency (which indicates the magnitude of the OGV loss) is greater for the engine across the outer third and inner third of the annulus, and about the same over the middle third. However, the higher OGV loss is offset by the generally higher rotor efficiency to yield an overall stage efficiency in the engine which is nearly identical to that measured on the Simulator.

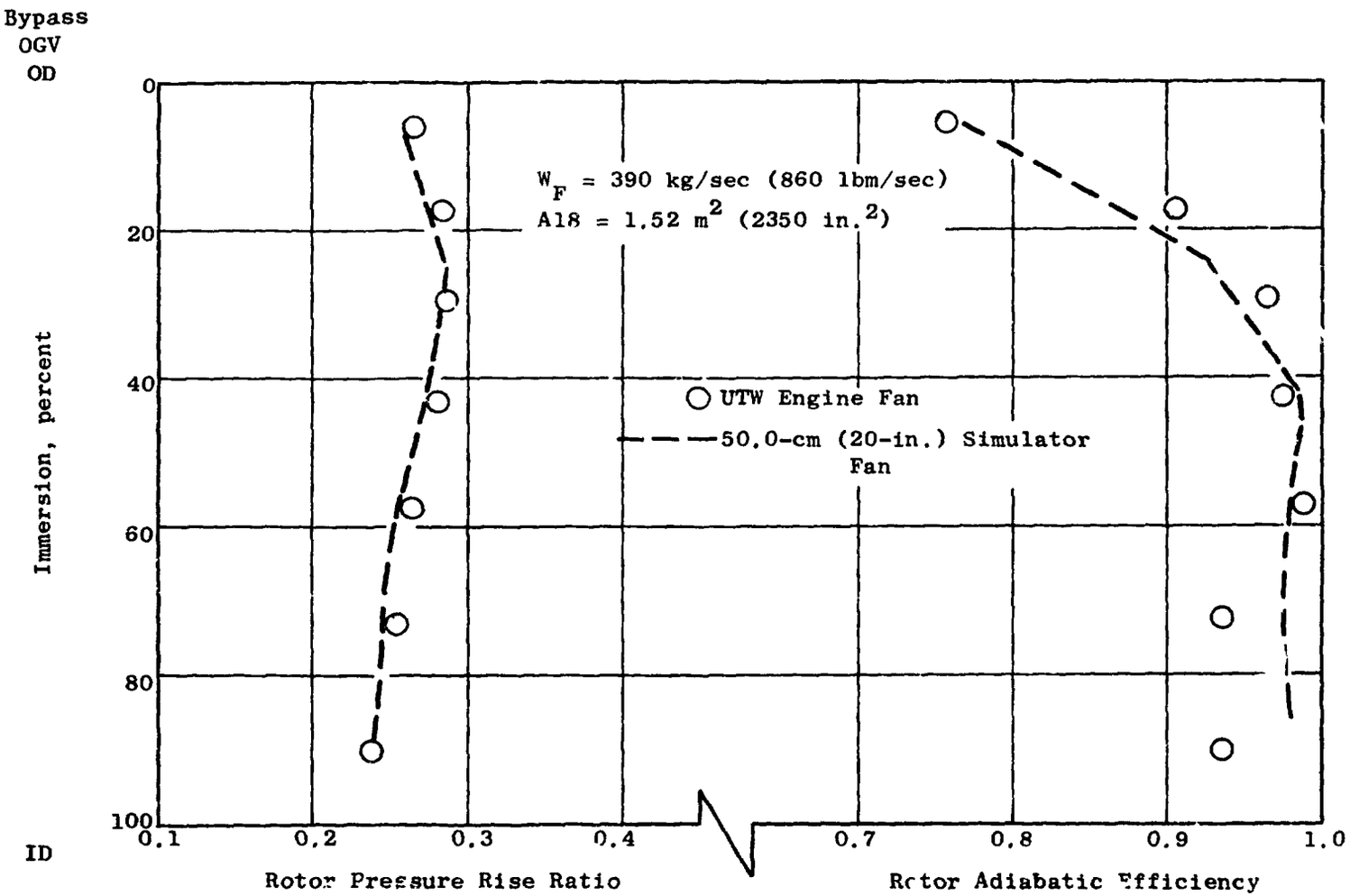

Figure 24. Rotor Bypass Pressure Rise Ratio and Efficiency Radial Profiles with β_F = 0° (Nominal) at 95% Fan Speed.

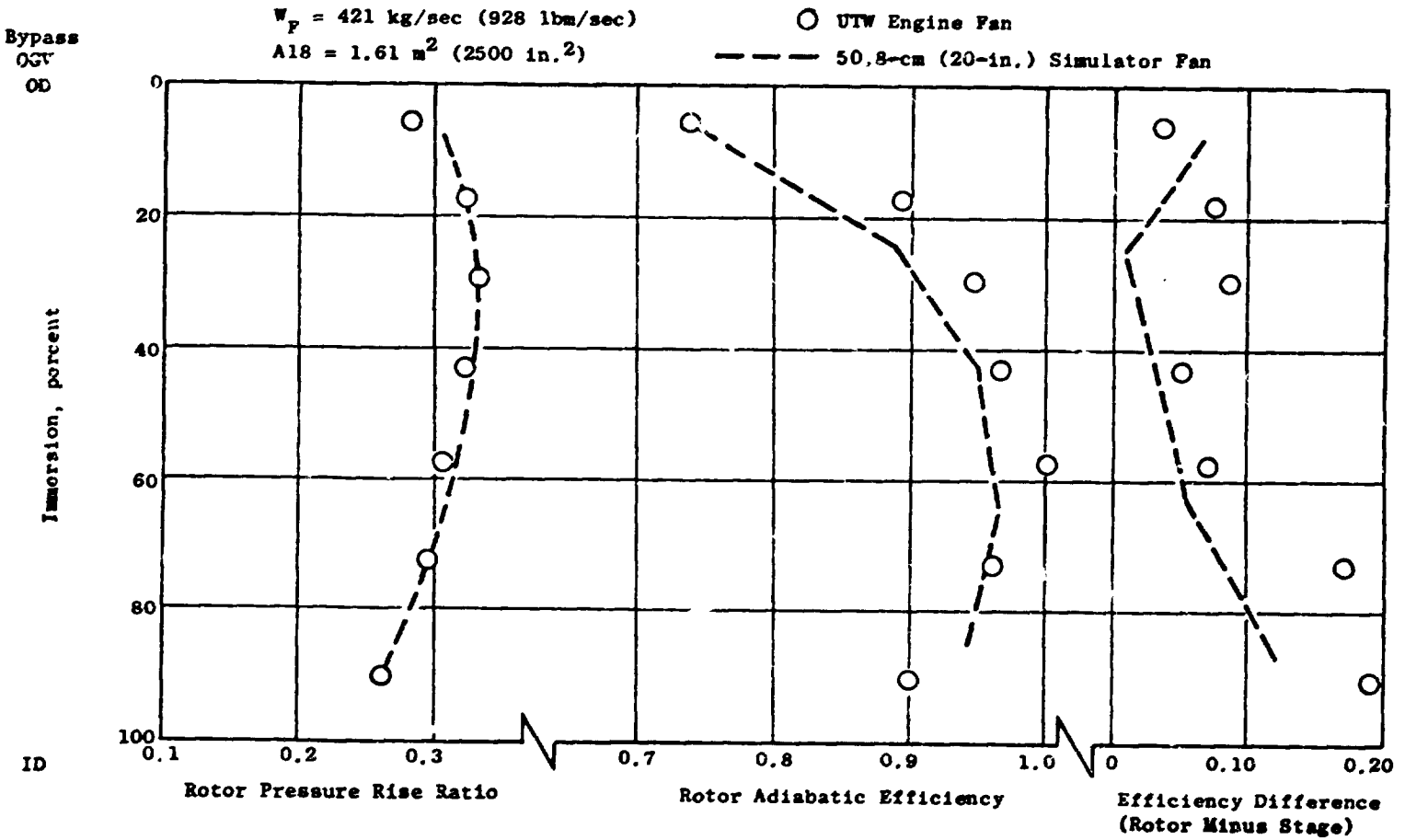

Figure 25. Rotor Bypass Pressure Rise Ratio and Efficiency Radial Profiles with β_F = -5° (Open) at 95% Fan Speed.

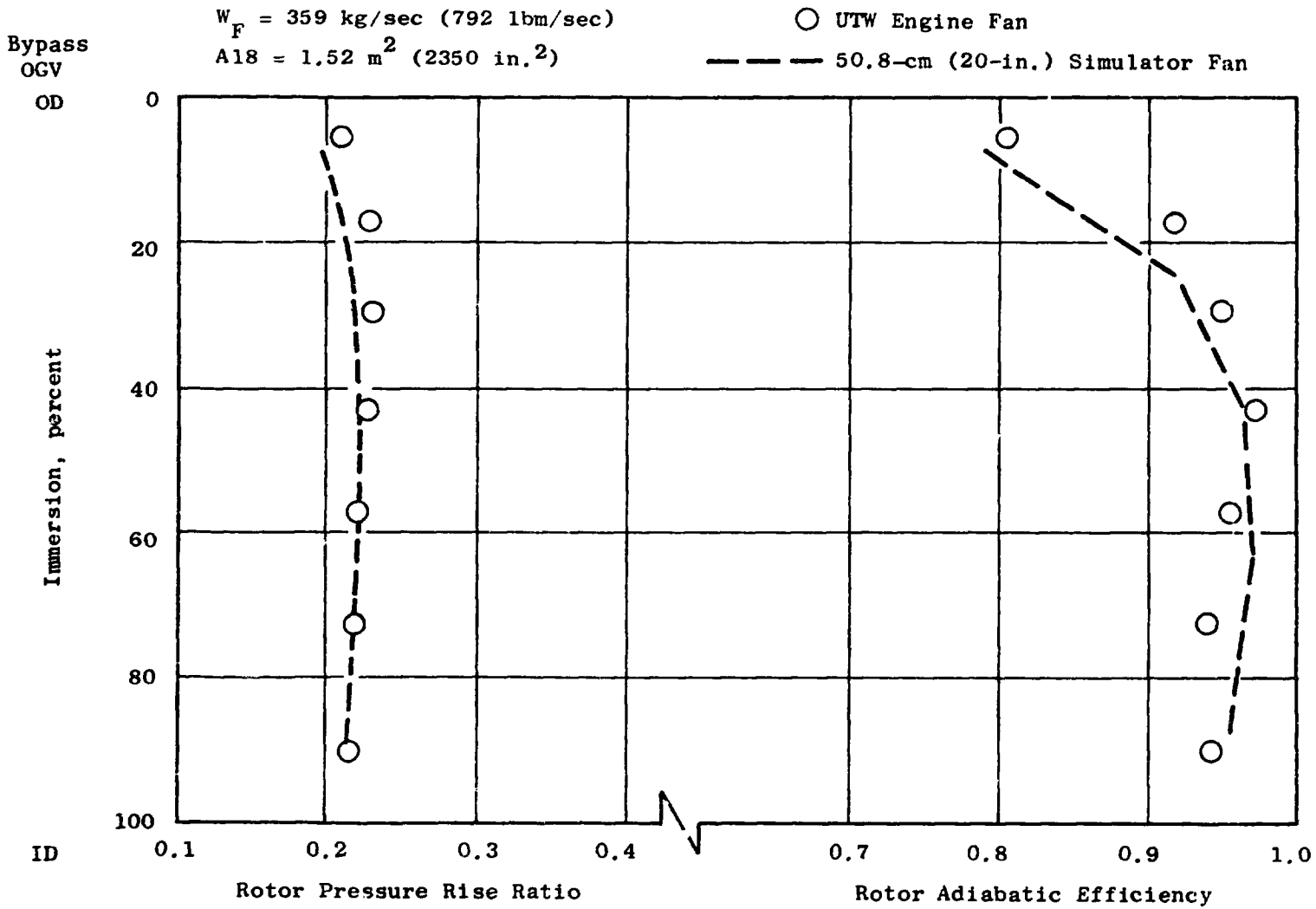

Figure 26. Rotor Bypass Pressure Rise Ratio and Efficiency Radial Profiles with β_F = +5° (Closed) at 95% Fan Speed.

4.1.6 Core Inlet Radial Profiles

Radial profiles of core inlet flow total pressure and temperature were measured by radial rakes located between struts in the transition duct. With the exception of the transition-duct-strut wake losses, these data define the inlet conditions to the core compressor. A comparison is made between the scale model profiles and the engine data in Figures 27 through 29 for the same representative high speed readings used in the rotor exit-profile comparisons of Section 1.4. A comparison of bypass ratios indicates that the core engine operated close to the assumed schedule that was used in the scale model tests, implying that similar flow-field patterns existed through the fan hub region and into the transition duct. In general, the engine pressure profiles measured slightly steeper gradients than the scale model and also measured higher average levels. The temperature-rise levels were higher in the engine, resulting in comparable fan-hub adiabatic efficiencies in both Simulator and engine.

4.2 REVERSE THRUST MODE

4.2.1 Overall Fan Performance

Test results obtained with the Simulator fan in the reverse thrust mode (Reference 3) indicated that the objective fan reverse thrust could be achieved with the rotor blades reversed through stall pitch. Reverse mode testing of the UTW engine was more limited and yielded insufficient data to fully define the fan's reverse mode performance, but the indication was that the engine could not produce the objective reverse thrust at the same fan speed and rotor blade pitch setting as demonstrated by the scale model. The engine data are shown in Figure 30 as fan pressure ratio (ratioed to ambient) versus total inlet flow (corrected to ambient conditions), and in Figure 31 as adiabatic efficiency versus inlet flow. These flow rates are rather approximate, however, since they were calculated from very limited measurements. A comparison with the cycle deck's predicted levels of pressure ratio and efficiency, derived from the Simulator test results, indicated that the engine fan performance was lower than expected. To determine the extent of the differences, radial traverse data taken in the inlet throat and aft duct were analyzed and are presented in the following sections.

4.2.2 Fan Rotor Discharge Flow-Field Characteristics

Reverse mode fan performance was evaluated from traverse data taken near the inlet throat, available only for one data point taken at 97% fan speed with the blades set at -105°. Based upon a radial integration of the total pressure, temperature, and swirl angle data, the following parameters were deduced: rotor discharge flow (corrected to Plane-15 conditions rather than ambient as in Figures 30 and 31), mass-weighted average pressure ratio, average temperature ratio, and fan thrust. Comparison with the 50.8-cm (20-in.) Simulator fan test results is tabulated and plotted in Figure 32.

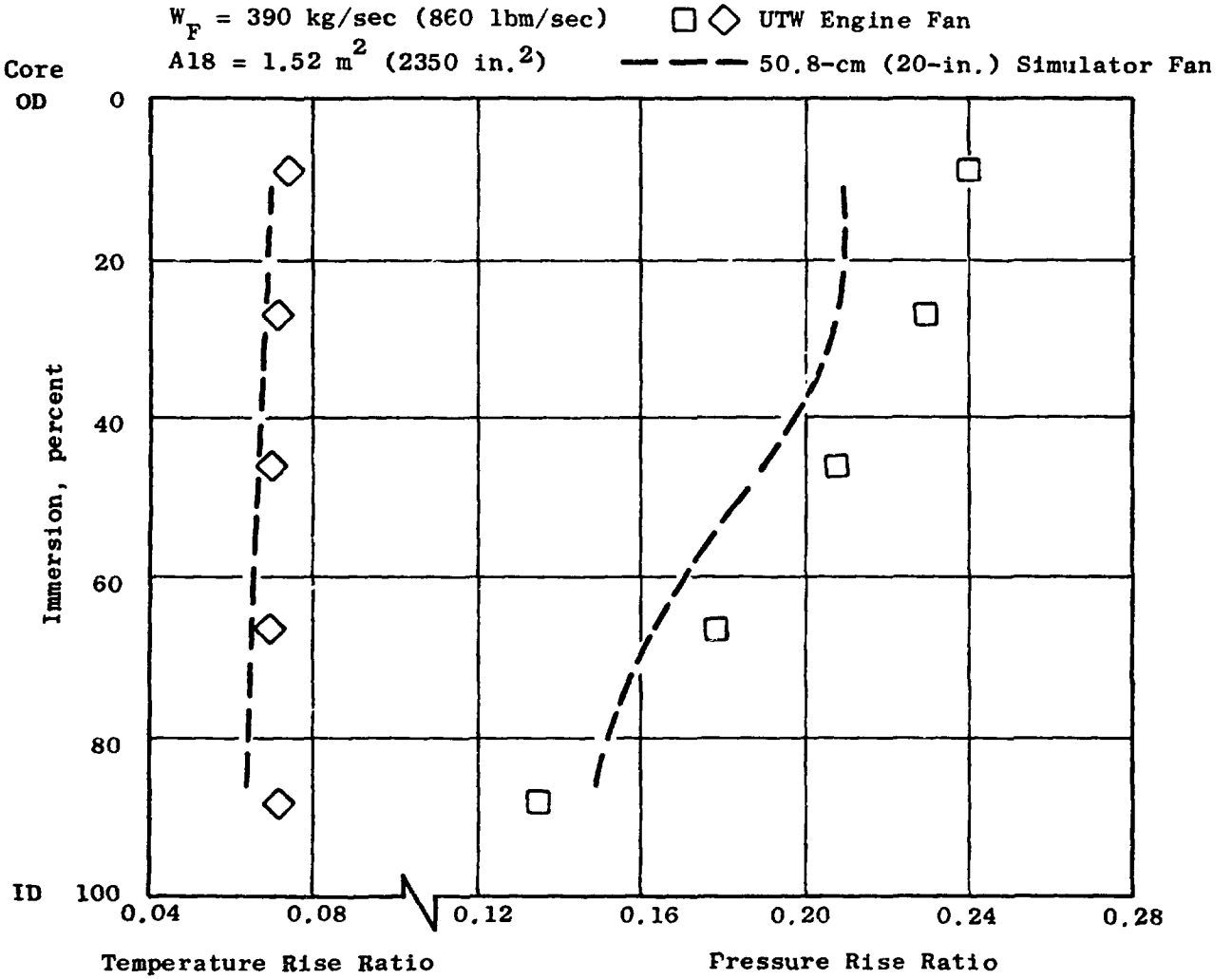

Figure 27. Core Inlet Pressure Rise Ratio and Temperature Rise Ratio Radial Profiles with β_F = 0° (Nominal) at 95% Fan Speed.

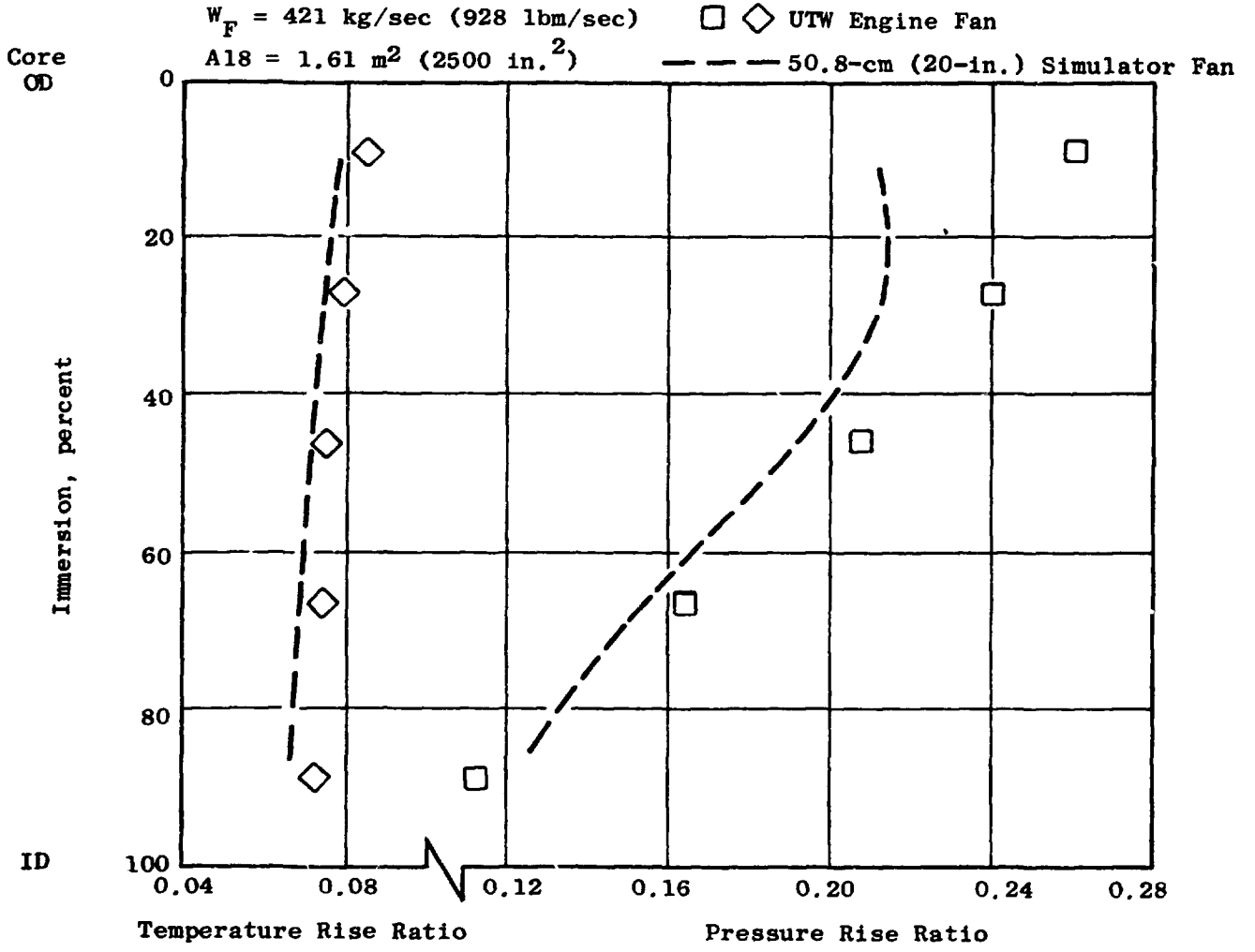

Figure 28. Core Inlet Pressure Rise Ratio and Temperature Rise Ratio Radial Profiles with β_F = -5° (Open) at 95% Fan Speed.

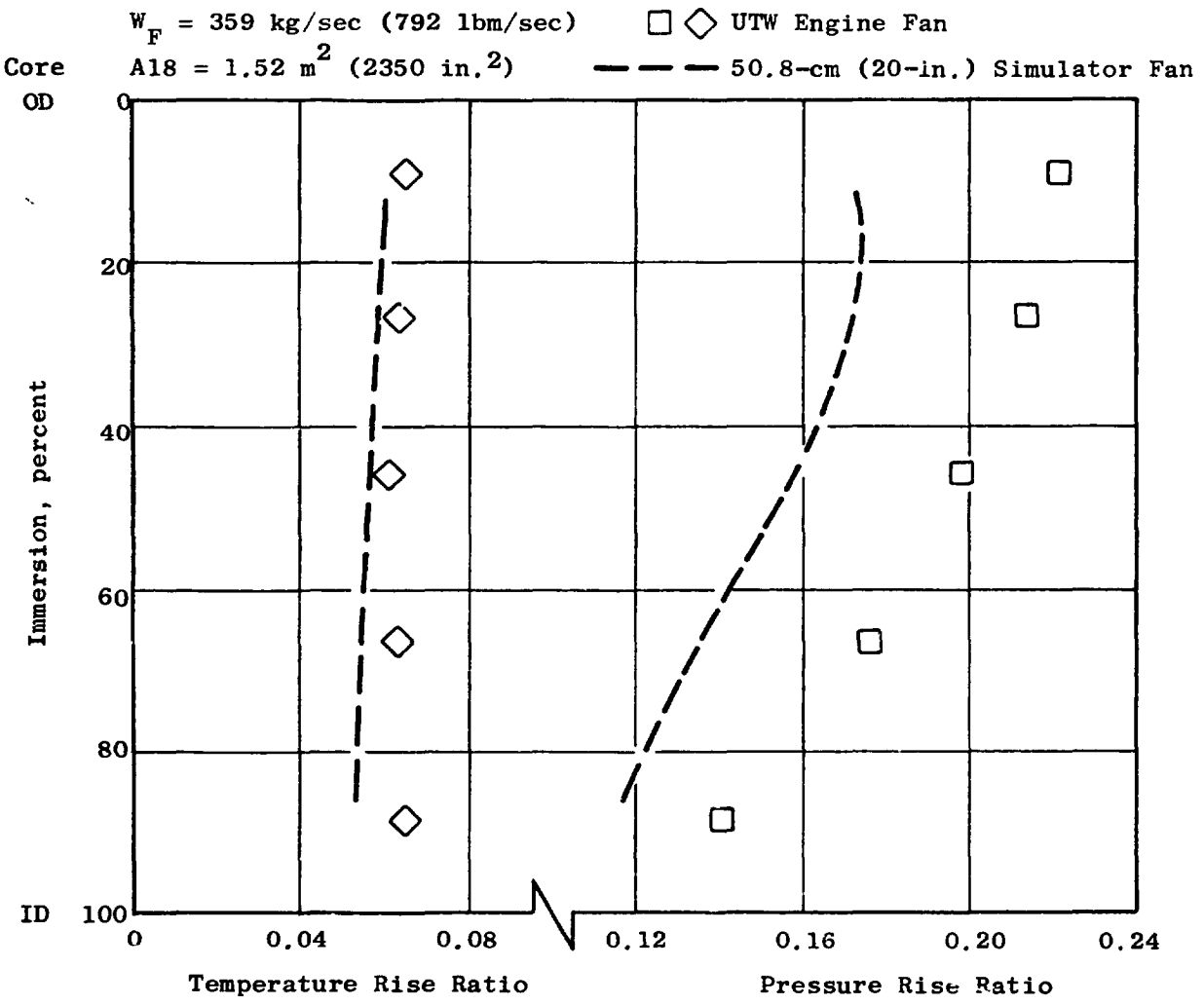

Figure 29. Core Inlet Pressure Rise Ratio and Temperature Rise Ratio Radial Profiles with β_F = +5° (Closed) at 95% Fan Speed.

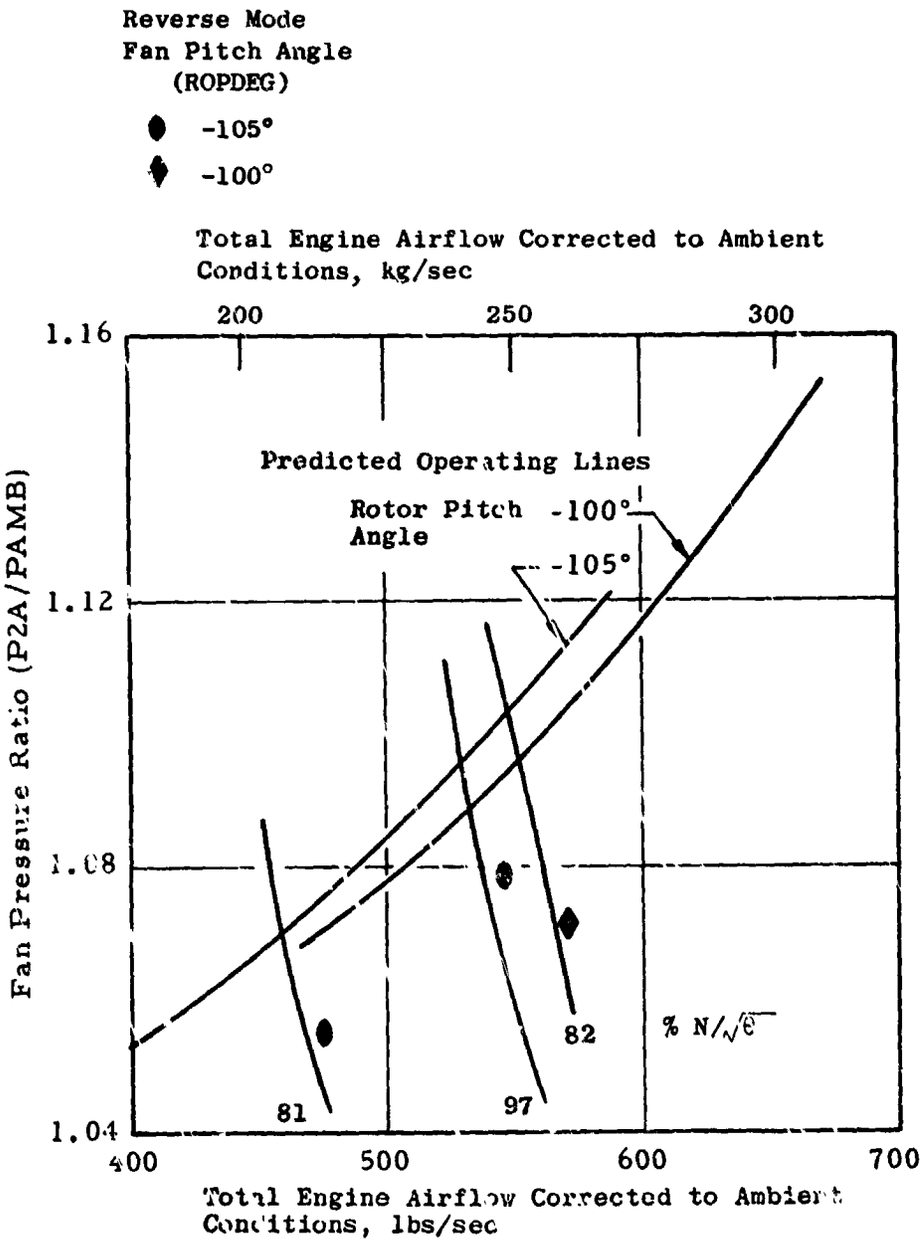

Figure 30. Fan Pressure Ratio Versus Airflow, Reverse Mode.

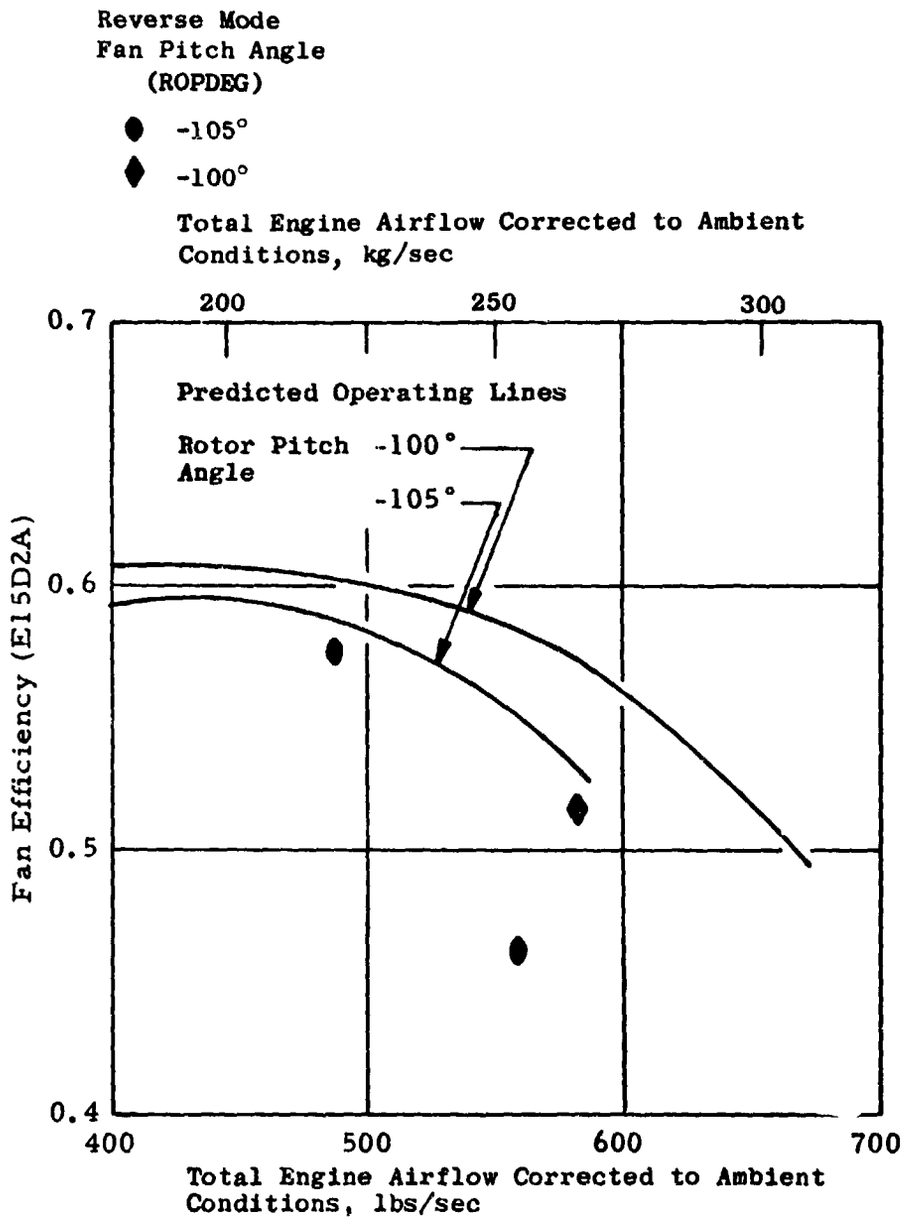

Figure 31. Fan Efficiency Versus Airflow, Reverse Mode.

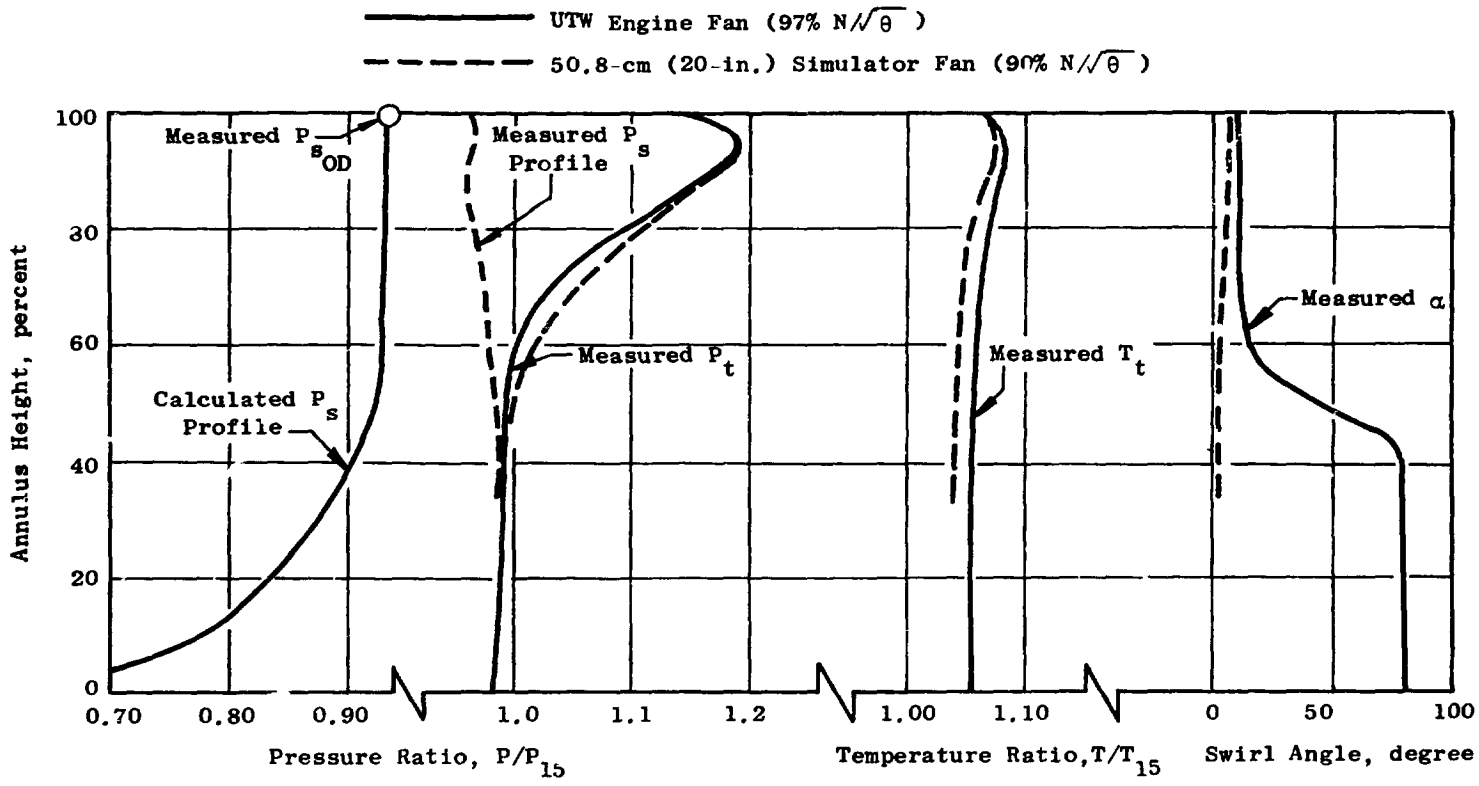

Summary of Results

	% $N/\sqrt{\theta_{15}}$	β	$(W\sqrt{\theta_{15}}/\delta_{15})_{Rotor}$	P/P_{15}	T/T_{15}	η
UTW Engine (Rdg 23i)	97	-105°	242 kg/sec (533 lbm/sec)	1.10	1.07	0.40
Interpolated from 20-in. Simulator Data	97	-105°	238 kg/sec (525 lbm/sec)	1.14	1.07	0.52

Figure 32. Reverse Mode Inlet Throat (Station 107) Traverse Data.

Note that for the Simulator, inlet-throat traverse data were only obtained at 90% fan speed. Thus, the magnitudes of the radial profiles in Figure 32 are not comparable, but the qualitative shapes are. The overall fan performance parameters, however, could be interpolated from the available Simulator data for the same condition tested in the engine. The tabulated summary in Figure 32 indicates that the rotor discharge flows agreed within 2%, and the temperature ratios (work input) were practically identical; but, the engine pressure rise was 27% lower, and the average discharge swirl from the engine fan was higher. Thus the engine fan thrust, as calculated from an integration of the traverse data, was significantly lower and consistent with the low level of net thrust recorded by the thrust meter.

The low thrust level of the engine fan, relative to the Simulator fan in the reverse thrust mode, is speculated to be a result of the geometry differences between the two vehicles. The incoming pressure distortion to the fan rotor due to the upstream acoustic splitter could produce radial shifts in the flow field that would change the fan-pumping characteristics. The fan rotor platform geometry and blade shape at the hub also were notably different between engine and scale model; there were rather large rakes in the inlet throat of the Simulator but not in the engine. Both of these differences may have caused a difference in the fan discharge effective-flow area. The engine's fan performance was consistent with what would be expected on a lower operating line, as if the effective discharge area was larger in the engine than in the scale model. Future reverse mode testing of the UTW fan should investigate the nature of the flow field at both rotor inlet and exit, and perhaps the acoustic splitter ring can be removed to assess its impact on the fan characteristics.

4.2.3 Exlet (Aft Duct) Flow-Field Characteristics

Significant geometric differences existed in the aft (bypass) duct between the UTW engine and the Simulator, in particular, the presence of an acoustic splitter in the engine duct that was not in the scale model. Traverse data for total pressure and total temperature were obtained across three-quarters of the annulus at two operating conditions, and the results are plotted in Figure 33. The pressure traverse indicated the expected localized region of high loss and blockage around the acoustic splitter. The temperature traverse measured higher values below the splitter (near the ID) than above, possibly indicating, some ingestion of core exhaust gases. Total inlet flow (corrected to Plane-15 conditions) was deduced from wall static pressures and a radial integration of the traverse data, and the results compared favorably with the 50.8-cm (20-in.) Simulator flow at similar conditions and with separate test results on a scale model of the exlet.

4.2.4 Core Duct Performance

As in the forward thrust mode, measurements taken by the radial rakes located between struts in the transition duct were used to evaluate core

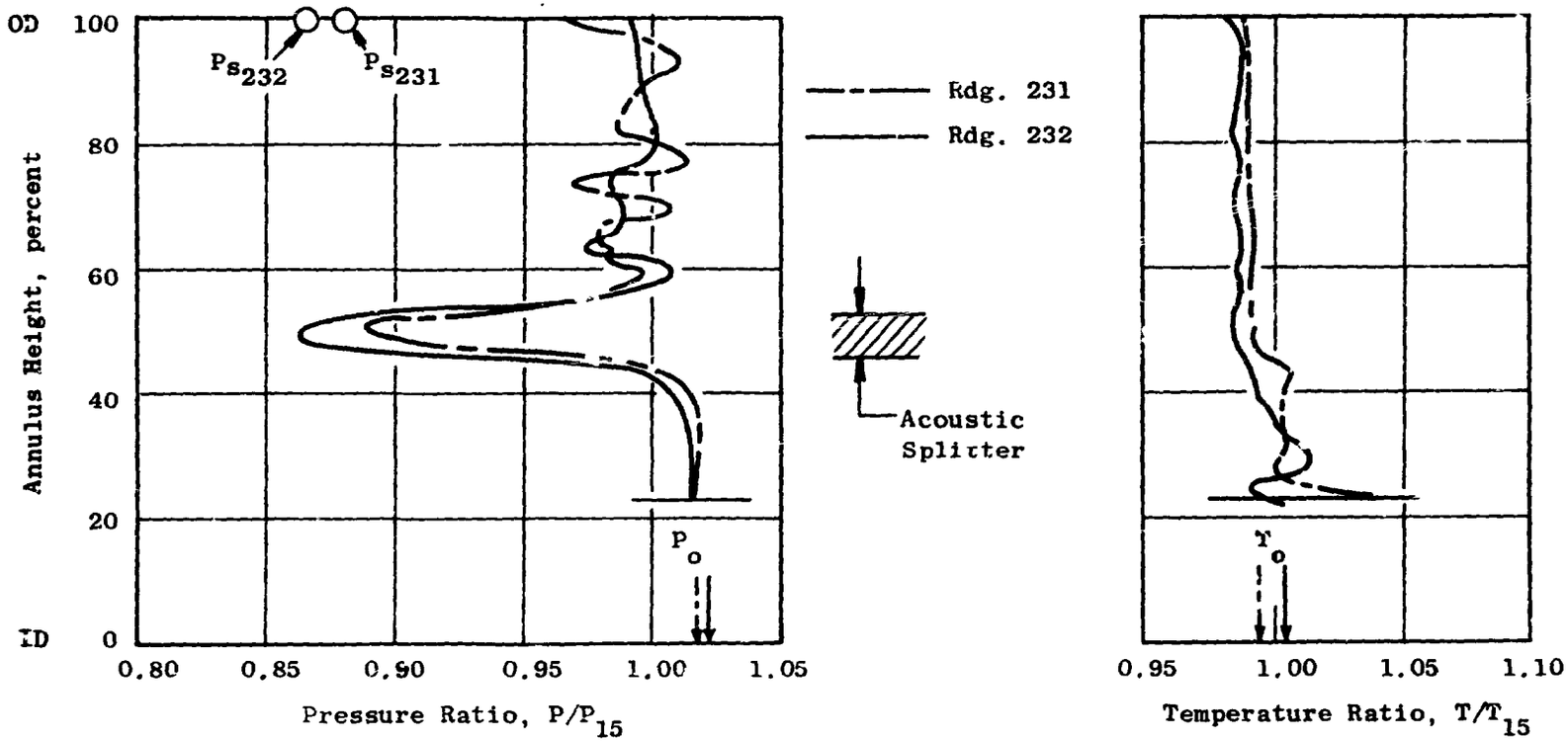

Summary of Results

% $N/\sqrt{\theta_{15}}$	β	UTW Engine ADH Reading	$(W\sqrt{\theta_{15}}/\delta_{15})$ Total Engine	$(W\sqrt{\theta_{15}}/\delta_{15})$ Total 20-in. Simulator	(P_{15}/P_o) Engine	(P_{15}/P_o) 20-in. Simulator
97	-105°	231	258 kg/sec (570 lbm/sec)	254 kg/sec (560 lbm/sec)	0.978	0.987
81	-100°	232	264 kg/sec (583 lbm/sec)	272 kg/sec (600 lbm/sec)	0.982	0.986

Figure 33. Reverse Mode Aft Duct (Station 204) Traverse Data.

duct performance. The total pressure recovery of the flow entering the core compressor is shown in Figure 34, comparing the limited engine data to the results of the 50.8-cm (20-in.) Simulator tests. As discussed in Reference 3, the recovery was found to be a function of the external momentum, or total fan flow, rather than of the core flow. Although slight differences existed between the two vehicles in the placement of the core inlet rakes and in the contour of the transition duct, the recovery characteristics of both are very similar. Apparently the engine core flow was not significantly affected by the losses associated with the acoustic splitter. The recovery levels measured in the scale model were recognized to be low, relative to design intent, but not low enough to be a limiting factor in producing the objective reverse thrust.

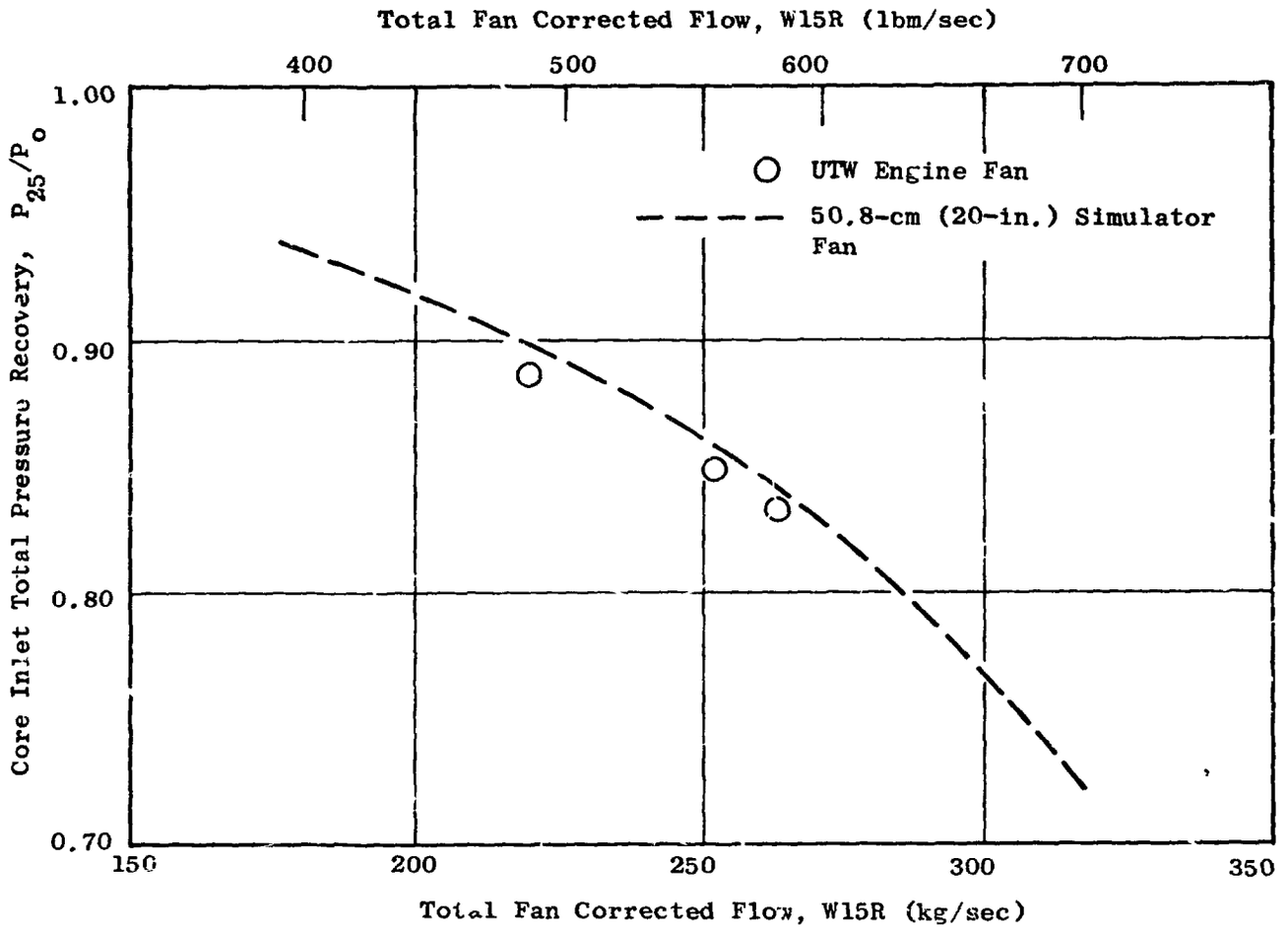

Figure 34. Core Inlet Total Pressure Recovery in Reverse Mode.

5.0 REFERENCES

1. The General Electric Company; "Quiet Clean Short-Haul Experimental Engine Under-the-Wing Final Design Report," NASA CR-134847, June 1977.

2. The General Electric Company; "The Aerodynamic and Mechanical Design of the QCSEE Under-the-Wing Fan," NASA CR-134842, September 1975.

3. The General Electric Company; "Aerodynamic and Aeromechanical Performance of a 50.8-cm (20-in.) Diameter, 1.34 PR, Variable-Pitch Fan with Core Flow," NASA CR-135017, August 1977.